M 2021

U.PORTO
FEUP FACULDADE DE ENGENHARIA
UNIVERSIDADE DO PORTO

DESIGN OF A LOGIC REACTOR FOR THE PRODUCTION OF METHANOL FROM BIOGAS

DÉBORA DE FIGUEIREDO LUIZ

DISSERTAÇÃO DE MESTRADO APRESENTADA
À FACULDADE DE ENGENHARIA DA UNIVERSIDADE DO PORTO EM
ENGENHARIA QUÍMICA

Master in Chemical Engineering

Design of a LOGIC Reactor for the Production of Methanol from Biogas

Master dissertation

of

Débora de Figueiredo Luiz

Developed within the course of dissertation

held in

DMT Environmental Technology

Supervisor at FEUP: **Prof. Alexandre Ferreira**

Coordinator at DMT: **Eng. Benny Bakker**

March 2021

Acknowledgment

First, to my mother, father, grandmother and brother, Claudia Luiz, Nelson Luiz, Maria das Dores and Daniel Luiz for all the help and support through all my life, for always believing in me and investing in my education.

To professor Alexandre Ferreira, supervisor of this dissertation, for all the constant help and support even with the distance between Portugal and The Netherlands.

To Eng. Benny Bakker, Eng. Maria Marcela Fragozo and Eng. Gerrit Wigger for the opportunity to develop my dissertation at DMT and for all the help with the project, but also for making sure all my opinions were respected and for making me fell part of the team since the beginning.

To my house and work mates, Maria Vendas, Sofia Sousa and Ana Cancela, for being a great company in Joure and making this period of the internship a lot more enjoyable.

To my friends Lívia Coutino and Paulo Marrocos, for the amazing friendship and all the help and support I could have needed during this semester, I do not know how I would have made it without you both.

To my friend Luisa Moreira, for being my first friend at FEUP and always making me feel welcome in Portugal, sharing her country's culture with me and always providing me with great adventures.

Last, but not least, my best friends in Brazil, Gabriella Francisco and Yasmim Monteiro for the over 12 years of friendship, for always being there for me and helping me with any problem I may have since school, without thinking twice.

Abstract

Nowadays, fossil fuel-based energy sources are the most used, but due to limited resources, they are destined to be over in a short future. To help solve this problem, one very promising alternative is methanol, as it can be used as fuel and energy carrier, since it is found in liquid phase under ambient conditions. Furthermore, methanol can be produced through renewable sources and decrease carbon emission by 65 to 95 % when compared to fossil sources.

Methanol is usually produced in two different types of gas phase catalytic reactors: adiabatic and isothermal. The main challenge regarding the design of a methanol reactor is the thermodynamic limitations of the overall synthesis reaction, which is known to cause low conversions and high recycle ratios. However, in 2015 a new reactor called LOGIC, which stands for liquid out gas in concept, was created and, in a lab study, it showed a capacity to generate high conversions and a methanol selectivity higher than 99.5 %.

The main goal of this thesis is to design a LOGIC reactor for the commercial production of methanol, this objective was set to be reached in two steps. The first one is to develop a full model and simulation, using MATLAB and Aspen Plus, of the three sections of the LOGIC reactor: catalytic, economizer and condenser. The second is to perform a comparative analysis by changing four distinct parameters in order to have the most efficient methanol production and design. These varied parameters consist in the catalytic reactor type, adiabatic or gas cooled; the presence or absence of baffles; the number of tubes, in a range from 500 to 2000 and, finally, the inlet temperature, varied between 513.15 K and 543.15 K.

After performing all the simulations and analyzing the results, the final design is a baffled gas cooled LOGIC reactor that presented the highest methanol production and conversion among all cases with 586 $kg\,h^{-1}$ and 7.7 %, respectively, and the lowest recycle ratio of 0.82. As for the dimensions, it contains 1000 tubes, accounting for an inner shell diameter of 3.7 m and a length of 5.9 m, considering only the catalytic and economizer sections. Moreover, the total inlet mass flowrate of the catalytic reactor is 1.63 $kg\,s^{-1}$, requiring only 0.27 $kg\,s^{-1}$ of fresh feed, also it needs 1072 kg of catalyst.

The development of this dissertation contributes to a better understanding on how to model and simulate a LOGIC reactor, it also opens a path for further improvement in its design in order succeed in the promising methanol market.

Keywords: Methanol production, LOGIC reactor, modeling, temperature control, reactor design.

Resumo

Atualmente, as fontes de energia obtidas a partir de combustíveis fósseis são as mais utilizadas, mas devido a recursos limitados estão destinadas a acabar num futuro próximo. Uma alternativa promissora para resolver este problema é o metanol, uma vez que pode ser usado como combustível e como transportador de energia, já que pode ser encontrado em fase líquida em condições ambiente. Para além disso, o metanol pode ser produzido a partir de fontes renováveis, sendo capaz de reduzir as emissões de carbono de 65 a 95 % quando comparado com as fontes derivadas de combustíveis fósseis.

O metanol é normalmente produzido através de dois tipos de reatores catalíticos em fase gasosa: adiabático e isotérmico. O maior desafio em relação à produção de metanol é a limitação termodinâmica da sua reação global de síntese, que causa baixa conversões e altas razões de reciclo. No entanto, em 2015 foi desenvolvido um novo reator chamado LOGIC, que significa, "*liquid out gas in concept*", ou seja, um conceito em que a entrada é feita em fase gasosa e a saída em líquida. Num estudo laboratorial, este reator foi capaz de produzir altas conversões e uma seletividade em relação ao metanol de mais de 99.5 %.

O objetivo da presente dissertação é projetar um reator LOGIC para a produção comercial de metanol, sendo que esta meta foi alcançada em duas etapas. A primeira trata-se do desenvolvimento do modelo e simulação, usando MATLAB e Aspen Plus, das três seções que constituem o reator: catalítica, do economizador e do condensador. A segunda parte passa por desenvolver uma análise comparativa variando quatro parâmetros, de forma a obter a produção de metanol e projeto do reator mais eficientes. Estes parâmeros são: tipo de reator catalítico, adiabático ou aquecido por gases; presença ou ausência de chicanas; número de tubos, que variam entre 500 e 2000 e a temperatura de entrada, que varia de 513.15 a 543.15 K.

Após analisar os resultados, o projeto final consiste no reator LOGIC arrefecido com o uso dos gases de reciclo e com a adição de chicanas. Este reator apresentou a maior produção de metanol e maior conversão, 586 $kg\,h^{-1}$ e 7.7 %, respetivamente, e a menor razão de reciclo, 0.82. Como principais dimensões, o diâmetro interno da carcaça, que contém 1000 tubos, é de 3.7 m e o seu comprimento é de 5.9 m, considerando apenas as secções catalítica e do economizador. Ademais, o caudal de entrada do reator catalítico é de 1.63 $kg\,s^{-1}$, que requer um caudal de alimentação de apenas 0.27 $kg\,s^{-1}$ e precisa de 1072 kg de catalisador.

O desenvolvimento desta dissertação contribui para uma melhor compreensão de como modelar e simular o reator LOGIC, abrindo caminho para posteriores aprimoramentos do seu projeto para obter sucesso no promissor mercado de produção de metanol.

Palavras-chave: Produção de metanol, reator LOGIC, modelagem, controlo de temperatura, projeto de reator

Declaration

I hereby declare, under word of honour, that this work is original and that all non-original contributions is indicated and due reference is given to the author and source

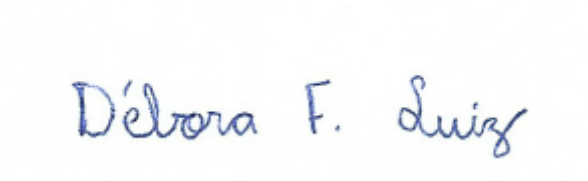

Débora de Figueiredo Luiz

08/02/2021

Index

List of Figures

List of Tables

Notation and Glossary

A_i	Inner transversal area of the tube	m^2
A_o	Outside lateral area of the tube	m^2
A_s	Minimum flow area in one baffle space	m^2
B_s	Baffle spacing	m
C	Clearance	m
Cp_g	heat capacity of the gas mixture	$J\,kg^{-1}\,K^{-1}$
D_h	hydraulic diameter	m
d_i	Inner diameter of the tube	m
d_o	Outer diameter of the tube	m
d_p	Diameter of the particle	m
D_s	Shell diameter	m
f_i	Friction factor inside the tube	
$f_{o,B}$	Friction factor in the shell side with baffles	
$f_{o,S}$	Friction factor in the shell side without baffles	
$h_{i,E}$	Tube side convective heat transfer coefficient for the economizer	$W\,m^{-2}\,K^{-1}$
$h_{i,PB}$	Tube side convective heat transfer coefficient in a packed bed	$W\,m^{-2}\,K^{-1}$
$h_{o,B}$	Shell side convective heat transfer coefficient in the economizer without baffles	$W\,m^{-2}\,K^{-1}$
$h_{o,S}$	Shell side convective heat transfer coefficient in the economizer with baffles	$W\,m^{-2}\,K^{-1}$
$h_{o,R}$	Shell side convective heat transfer coefficient in catalytic reactor	$W\,m^{-2}\,K^{-1}$
j_i	Colburn j-factor for an ideal tube bank	
K_{eq}	Thermodynamic equilibrium constant	
k_f	Thermal conductivity of the gas mixture	$Kg\,m^{-1}\,s^{-1}$
k_i	kinetic constant i	
k_{ij}	Binary interaction parameter between the components I and j	
k_w	Thermal conductivity of the tube wall	$Kg\,m^{-1}\,s^{-1}$
L_E	Length of the economizer	m
L_R	Length of the catalytic reactor	m
L_t	Length of the catalytic and economizer sections together	m
$\dot{m}_i$	Mass flowrate inside one tube	$Kg\,s^{-1}$
$\dot{m}_o$	Mass flowrate in the shell side	$Kg\,s^{-1}$
M_T	total mass flowrate inside the tubes	$Kg\,s^{-1}$
MW	Molecular weight	$Kg\,mol^{-1}$
N_t	Number of tubes	
P	Pressure	Pa, bar
$P_{c,i}$	Critical pressure of the component i	bar
$p_{f,i}$	Polarity factor of the component i	
p_i	Partial pressure of the component i	bar
P_{in}	Inlet pressure	Pa, bar
Pr	Prandtl number	
P_R	Pitch ratio	
P_t	Tube pitch	m
Q	Heat duty of the economizer	W
$\mathrm{Re_B}$	Shell side Reynolds number in the economizer with baffles	
$\mathrm{Re_D}$	Shell side Reynolds number in the economizer without baffles	
$\mathrm{Re_i}$	Tube side Reynolds number	
r_i	Rate of the reaction i	$mol\,kg^{-1}\,s^{-1}$
$\mathrm{R_g}$	Universal gas law constant	$J\,mol^{-1}\,K^{-1}$
SN	stoichiometric number	
T	Temperature	K, °C

T_b	Bulk temperature	K
$T_{c,i}$	Critical temperatures	K
T_{in}	Inlet temperature	K
T_{out}	Outlet temperature	K
$T_{R,i}$	Reduced temperature	
T_{shell}	Shell temperature	K
U_{shell}	Overall heat transfer coefficient inside the shell	$W\,m^{-2}\,K^{-1}$
U_{tube}	Overall heat transfer coefficient inside the shell	$W\,m^{-2}\,K^{-1}$
V	Specific volume	m^3
v_i	Velocity of the gas inside the tube	$m\,s^{-1}$
v_o	Velocity of the gas inside the shell	$m\,s^{-1}$
W_{cat}	Catalyst weight	kg
w_i	Acentric factor	
y_i	Mol fraction of the component i	
z	Axial coordinate	m
Z	Compressibility factor	

Greek Letters

ε_b	Bed voidage	
μ_g	Viscosity of the gas mixture	$kg\,m^{-1}\,s^{-1}$
ρ_b	Density of the bed	$kg\ m^{-3}$
ρ_{cat}	Catalyst particle density	$kg_{cat}\ m^{-3}$
ρ_g	Density of the gas mixture	$kg\ m^{-3}$
ΔH^r	Reaction enthalpy	$kJ\,mol^{-1}$
ΔP_i	Pressure drop inside the economizer's tube	Pa
$\Delta P_{o,B}$	Pressure drop in the shell side of the economizer with baffles	Pa
$\Delta P_{o,S}$	Pressure drop in the shell side of the economizer without baffles	Pa
ΔT	Temperature difference	K
ΔT_{LMTD}	Mean logarithmic temperature difference	K
ν	Stoichiometric coefficient	
ω_i	Mass fraction of the component i	

List of Acronyms

AR	Adiabatic reactor
CO	Carbon monoxide
CO_2	Carbon dioxide
CH_3OH	Methanol
CH_4	Methane
DMT	*Dirkse Milieu Technologie*
FF	Fresh feed
GCR	Gas cooled reactor
H_2	Hydrogen
LOGIC	Liquid out gas in concept
MATLAB	Matrix laboratory
NC	Number of components
NOx	Nitrogen oxides
NR	Number of reactions
TEMA	Tubular Exchanger Manufacturers Association
VLE	Vapor–liquid equilibrium

1 Introduction

1.1 Framing and Presentation of the Work

Nowadays, oil, natural gas and coal are the main sources of energy, but these resources are limited and are destined to be over within three centuries, because of that, making investments in renewable pathways to produce energy is crucial. However, creating a new energy source is not the only problem, its storage must be considered as well, that is why methanol has been studied as a feasible solution for both problems and it can serve as raw material as well. Besides that, methanol can be produced with renewable sources, which can favor the transition away from fossil fuels. (Olah, 2005; Bertau *et al.*, 2014)

Furthermore, methanol is found in liquid phase under ambient conditions and is considered the world's most shipped chemical commodity with more than 95 billion liters manufactured every year. It has been stored, transported and handled safely for over 100 years which is an advantage compared to other potential alternative fuels such as ammonia or hydrogen. As methanol can be reversely converted into hydrogen and become an energy carrier for it, solving its storage and transportation problem.(Márquez, 2018; Palmer and Floyd, 2020)

However, the main use of methanol nowadays is feedstock for a large variety of chemicals like formaldehyde, which consumes around 70 % of methanol produced worldwide, followed by methyl tert-butyl ether with 20 % , and the rest used for acetic acid and dimethyl ether. Additionally, it can also be employed as an intermediate in manufacturing many products such as paints, resins, silicones, adhesives, antifreeze and plastics.(Dalena *et al.*, 2018)

Methanol itself can be used directly as fuel as it has an octane number of 113, but its energy density is about half of gasoline, which presents an octane number of 100, so a strategy of mixing both fuels is promising. Some mixtures, already available in the market, are M85 (85 % methanol, 15 % gasoline) and M100 (100 % methanol), the last one being less common. Besides the advantage of methanol improving engine performance by lowering its combustion temperature, it also reduces emissions of NOx when compared to conventional fuels.(Olah, 2005; Bozzano and Manenti, 2016)

Although approximately 66 % of methanol is still produced from fossil sources like natural gas and coal, methanol produced through renewable sources has been studies and implemented lately. For instance, biogas and renewable hydrogen from water electrolysis is a viable way to produce methanol and can reduce carbon emissions by 65 to 95 % when compared to fossil origin-based ones.(Bertau *et al.*, 2014; Márquez, 2018)

1.2 Presentation of the Company

DMT stands for *Dirkse Milieu Technologie* after the founder Rob Dirkse in 1987. "*Milieu Technologie*" means Environmental Technology, after internationalization, it became DMT Environmental Technology. (DMT Environmental Technology, 2021)

Figure 1: Places where DMT has systems running. (DMT Environmental Technology, 2021)

DMT International holds DMT Environmental Technology and DMT Clear Gas Solutions with over 100 employees and partners spread throughout Europe, North America and Asia, as it can be seen in Figure 1. The company develops technology supplier for biogas to renewable natural gas and H_2S removal technologies with systems already running in over 20 countries. (DMT Environmental Technology, 2021)

1.3 Contribution of the Author to the Work

This dissertation is the first one made over the development of the LOGIC reactor at DMT Environmental Technology, it was based on the academic work of M.J. Bos and D.W.F. Brilman (2015) and adapted to be able to produce methanol in commercial scale.

The main contributions for this work are:

1. The upscale production of methanol achieved by changing the reactor to a multi-tubular design and modeling it as the two main types of gas phase methanol reactors available in the market, adiabatic and quasi-isothermal gas cooled.
2. The addition of the economizer section so the reactor would work by means of natural convection, introducing the concept of heat exchanger design.

3. The development and availability of the MATLAB codes used to simulate the catalytic reactor and the economizer, as they can be used as base for future improvement and to simulate the production of methanol at different scales.
4. A comparative analysis to help understand the impact of four parameters, such as catalytic reactor type, presence of baffles in the economizer, number of tubes and inlet temperature in the design of a LOGIC reactor.

1.4 Organization of the Dissertation

This Master Thesis is organized into 6 chapters. The main purpose of each chapter is briefly described as follows:

Chapter 1 provides a framework of the current scenario regarding methanol production and its demand; Presents the company, DMT Environmental Technology; states the main contribution of the author over the thesis' subject.

Chapter 2 is the state of art, it describes which technologies have been used to produce methanol and introduces a new reactor called LOGIC, which stands for liquid out gas in concept and is the one this thesis was based on.

Chapter 3 consists of a description of the equations and assumptions used to model the LOGIC reactor, as well as an explanation of how the programs used to simulate it works.

Chapter 4 contains the results and discussion of a comparative analysis made in order to decide which design would be the most efficient to produce around 525 $kg\,h^{-1}$ of methanol with the LOGIC reactor.

Chapter 5 is the conclusions taken from all the data analyzed and a resume of the main goals achieved during the project.

Chapter 6 includes the degree of accomplishments of the objectives and suggestions for future works considering the limitations encountered

2 Context and State of the Art

Methanol is the simplest of the organic compounds called aliphatic alcohols, originally produced from destructive distillation of wood. It is, also, a colorless liquid, in ambient conditions, volatile, highly toxic for human consumption and flammable, burning with an almost invisible flame (OTT et al., 2012). Because of these factors, its production has to be made in a safe way, while still keeping the process efficient. This chapter will discuss the different types of methanol reactors commonly used, as well as a new promising technology.

2.1 Types of Methanol Reactors

To keep up with the global demand for methanol, the reactors used for its synthesis are in constant improvement. Currently, the production of methanol is mainly achieved through gas phase reactors, which can be either adiabatic or isothermal. (Leonzio, 2018)

The production of methanol presents some aspects that must be considered. For example, the thermodynamic equilibrium that favors the methanol formation when the temperature is low and pressure is high, since the overall synthesis reaction is exothermic and followed by a decrease of the total number of moles. However, these conditions are known to decrease the rate of reaction due to the kinetics limitations, leading to an impasse. Consequently, the main challenge in the reactor design is to have the most efficient temperature control to obtain the highest conversions and lowest recycle rations while keeping the costs as low as possible. (Ott *et al.*, 2012)

2.1.1 Adiabatic Reactors

Concerning adiabatic reactors, quench converters have been the most used for methanol synthesis for more than 40 years, it consists in a series of adiabatic catalyst beds inside a pressurized bed. This type of reactor is commonly used in smaller scales and the main advantage is that it offers easy design and operation for a low cost.(Alarifi et al., 2015)

The problems with the adiabatic reactor concern the poor temperature control inside it, as high temperature profiles are developed causing catalyst deactivation due to sintering, especially at temperatures above 550 K. Consequently, this scenario leads to low conversions, high recycle streams and shortening of the catalyst's lifetime. Another issue that happens in some of the adiabatic reactor configurations is the irregular flux distribution due to variable void fraction along the bed, that leads to different temperature zones inside the bed.(Bertau *et al.*, 2014)

Through all the years, some design optimizations were made as an attempt to improve temperature control. Most of them consist in implementing radial flow through catalyst bed and improving gas redistribution and heat recovery. However, these solutions require more complicated design and tuning, besides being more expensive, which goes against the main reasons why adiabatic reactors are used. Figure 2 is an overview of the most used methanol adiabatic reactors. (Bozzano and Manenti, 2016)

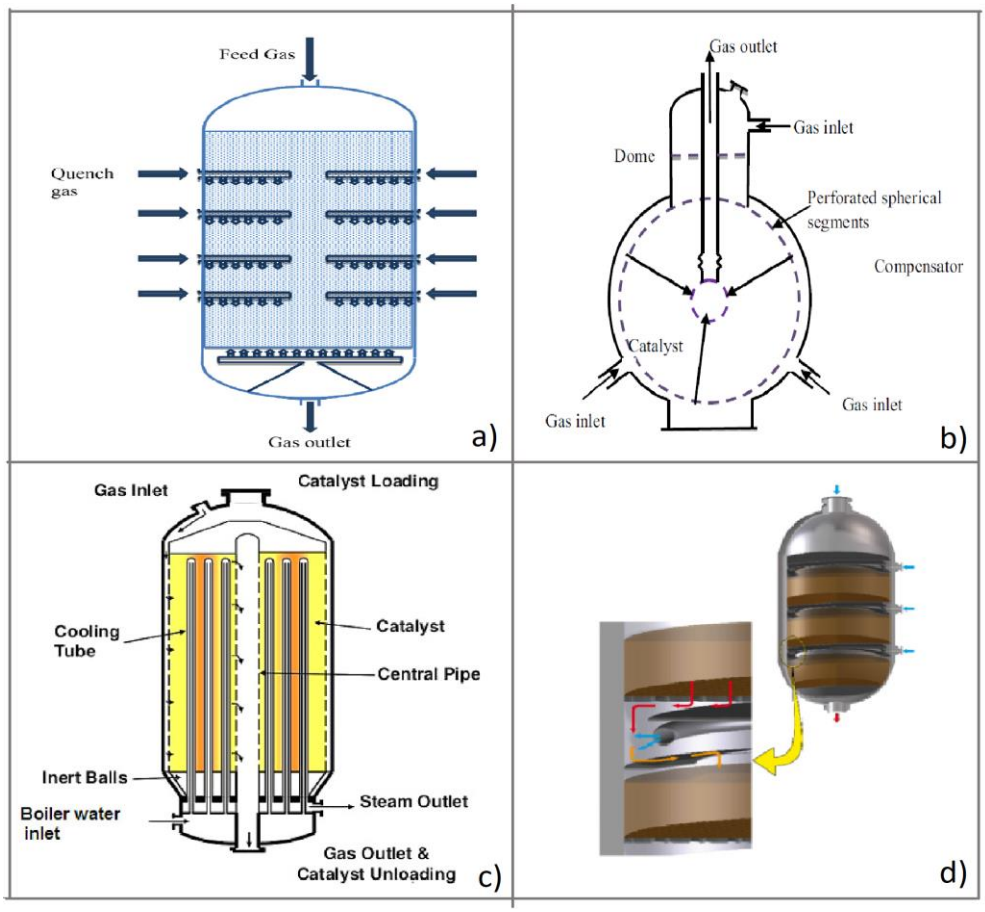

Figure 2 : Different types of adiabatic reactors: a) Quench reactor b) Spherical reactor c) Toyo MRF-Z® reactor d) ARC technology. (Bozzano and Manenti, 2016)

2.1.2 Isothermal Reactors

The isothermal reactor concept was developed as an effort to lower the temperature inside the reactor and keep it as constant as possible, all of this by means of cooling strategies such as gas-cooling and boiling water, resulting in a quasi-isothermal process. This design provides longer lifetime for the catalyst, higher yield due to the equilibrium favoring, fewer byproducts and high energy recovery through the coolant. Due to all these benefits, this configuration is the most applied in large scale units. The isothermal reactors available in the market provide different ways to enhance temperature control through heat exchange strategies.(Leonzio, 2018)

The first example of this type of technology is the Linde reactor, Figure 3b), which has multilayered helically coiled tubes filled with boiling water inside of the catalyst bed, providing indirect heat exchange. (Bozzano and Manenti, 2016)

The Lurgi reactor, Figure 3c), is a fixed bed shell and tube design with the catalyst inside the tubes and boiling water in the shell, the temperature is manipulated by steam pressure control. When larger capacity plants are desired, it is possible to use two Lurgi methanol converters, the first one is small and operates at high space velocities and temperatures in order to achieve only partial conversion, allowing to produce high-pressure steam. The outlet of the first reactor is fed to the second, but in the shell side and it flows in countercurrent with the cold fresh gas inside the tubes.(Tijm, Waller and Brown, 2001)

Mitsubishi Gas Chemical and Mitsubishi Heavy Industry developed a superconverter, Figure 3a). It is a type of a shell and tube reactor, but the tubes are double walled with the catalyst loaded in the space between the outer and inner tubes. The gas is fed at the bottom in the inner part of the tube, when it reaches the top of the reactor it flows downwards where the catalyst is, all of this while the cooling water flows in the shell side. This design works in a way that the catalyst bed temperature is higher near the inlet, but gradually lowers toward the outlet exchanging heat with the feed gas. Mitsubishi assures that the superconverter provides safe operation and a high level of mechanical stability.(Matsumoto et al., 1997)

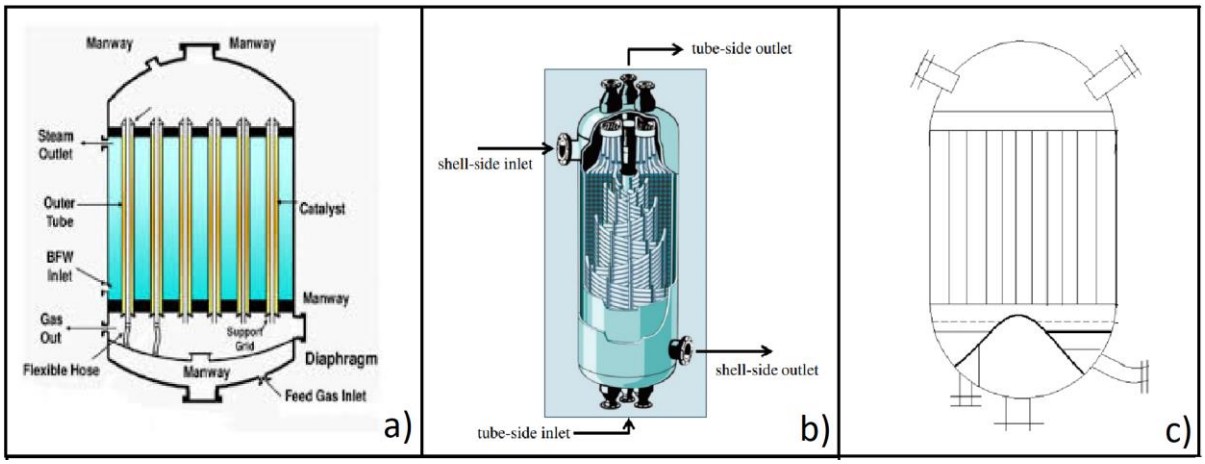

Figure 3: Different types of isothermal reactors: a) Mitsubishi superconverter, b) Linde reactor and c) Luigi reactor. (Bozzano and Manenti, 2016)

2.2 A New Methanol Reactor Concept

In 2015, an article developed by M.J. Bos and D.W.F. Brilman (2015) introduced a new reactor called LOGIC, which stands for liquid out gas in concept and this name is attributed

because the reactants are entered as gases and the desired products are collected in liquid form.

This new design consists in a reactor with two different temperature zones. Firstly, the reactant gases CO_2 and H_2 are introduced in the hot zone at the bottom of the reactor, called catalyst section, where the reaction occurs. After that, the products enter the cold zone at the top, the condenser section, where methanol and water are condensed and removed in liquid form and the unreacted gases are recirculated to the catalyst section. Given the disposition of the zones, the gases circulate inside the reactor by means of natural convection. (Bos and Brilman, 2015; Bos *et al.*, 2019)

The main advantages of this configuration, according to Bos *et al.* (2019), are that the reactor operates autothermically, generates a full carbon conversion and a methanol selectivity higher than 99.5 % on carbon basis. In Figure 4a there is a picture of the lab unit of the LOGIC reactor located at the University of Twente in The Netherlands that produced 0.2 kg day^{-1} of methanol and in Figure 4b a schematic overview of it.

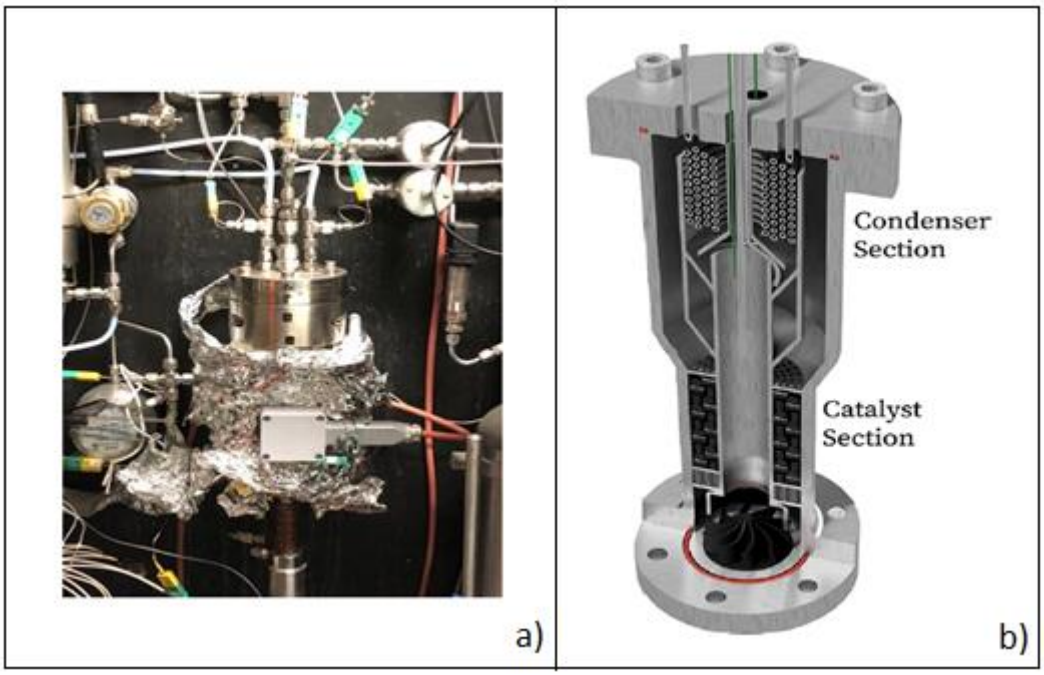

Figure 4: Logic reactor: a) Laboratory unit and b) schematic view (Bos et al., 2019).

As a next step on the development of this technology, in the beginning of 2020, DMT started a consortium with UT Twente, ISPT and Shell to create a pilot unit to produce around 15 kg day^{-1} of methanol from CO_2 by adding renewable hydrogen using the LOGIC reactor. The project is expected to be ready by the end of 2022.

In order to make the reactor able reach this production, some changes were proposed, one of them is the addition a new section called economizer. It consists in a shell and tube heat exchanger in which the hot fluid in the tube side is the gaseous products coming out of the

catalyst section and the cold fluid in the shell side is the unreacted gases coming from the condenser section. This part is designed in such a way that the reactor can operate in natural convection, using the gravity and density difference to do so. Another modification is turning the catalytic reactor into a multi-tubular layout to improve the methanol production and the heat transfer mentioned above.

The next step to consolidate this new technology is to produce around 525 kg h^{-1} of methanol using the LOGIC reactor, which is the goal of this master thesis.

3 Materials and Methods

As mentioned, the current LOGIC reactor design consists in three sections combined in the vertical direction. In the catalytic section, the reactor will be modeled as a multi-tubular adiabatic reactor, AR, and as a gas cooled reactor, GCR, to verify which of the main types of gas phase reactors would be the most efficient. The economizer section will also be modeled in two ways, both as single pass shell and tube heat exchanger, but one will be with and the other without baffles. Both of these were implemented in MATLAB. Finally, the condenser section will be done using a Flash Vessel in Aspen Plus.

Figure 5 is a flowsheet format of how the LOGIC reactor works for better understanding and also how it will be modeled.

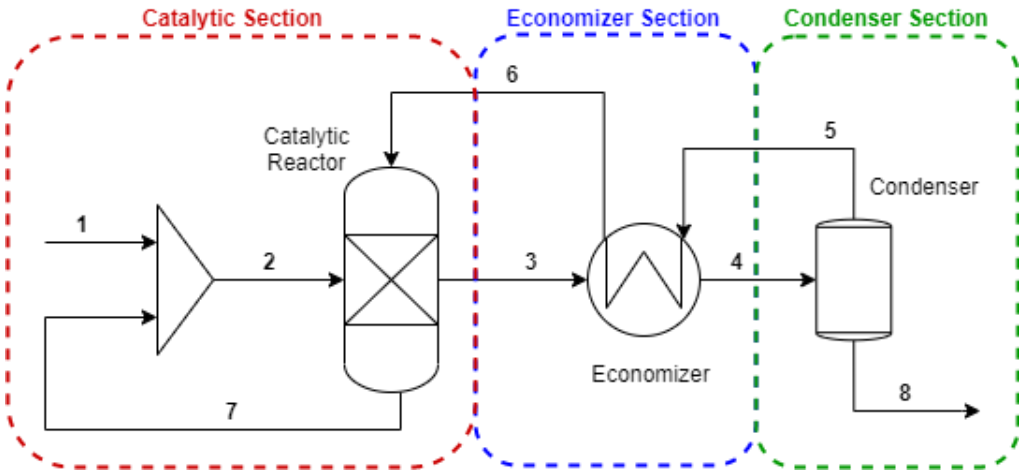

Figure 5: LOGIC reactor in a flowsheet format.

The process starts with stream 1, the fresh feed, mixing with stream 7, which is composed by the recycled gases after all the heat was exchanged, resulting in the stream 2, the inlet of the catalytic reactor inside the tubes. Stream 3 is the outlet of the reactor that enters the heat exchanger also in the tube side and leaves as stream 4, being the inlet of the flash vessel. Stream 8 is the liquid outlet of the flash that contains the desired product, methanol, and stream 5 is the vapor one that enters the heat exchanger in the shell side and leaves it as stream 6, entering the reactor in the shell side.

As the reactor is multi-tubular, it is necessary to define the arrangement of the tubes inside the shell, as it influences the heat exchange.

According to Sadik Kakaç, Hongtan Liu (1998), the tubes laid in a triangular layout with 30° angle results in the greatest tube density, which means more area per unit volume of shell. The tube pitch, P_t, is the shortest distance between the center of the tubes, it is usually 1.25 to 1.5 the outside diameter of the tube. The shortest distance between the outside diameter,

d_o, of 2 tubes is called clearance, C. A representation of the tube layout can be seen in Figure 6.

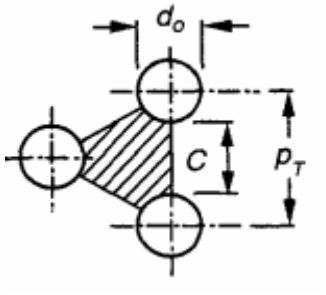

Figure 6: 30° triangular pitch tube layout. (Sadik Kakaç, Hongtan Liu, 1998)

3.1 Catalytic Section

3.1.1 Methanol Synthesis

Regarding methanol synthesis, three overall reactions are possible, the hydrogenation of CO, the hydrogenation of CO_2 and the reverser water-gas shift reaction, given by Equations 1, 2 and 3, respectively. These three are not independent, and any one of them can be expressed as a linear combination of the other two.(Ott *et al.*, 2012)

$$CO + 2H_2 \leftrightarrow CH_3OH \qquad \Delta H^r_{298} = -90.8\ \text{kJ mol}^{-1} \tag{1}$$

$$CO_2 + 3H_2 \leftrightarrow CH_3OH + H_2O \qquad \Delta H^r_{298} = -49.2\ \text{kJ mol}^{-1} \tag{2}$$

$$CO_2 + H_2 \leftrightarrow CO + H_2O \qquad \Delta H^r_{298} = +41.2\ \text{kJ mol}^{-1} \tag{3}$$

Where ΔH^r_{298} is the reaction enthalpy of each of the reactions at 298 K.

3.1.2 Reactor Feed Composition

The fresh feed, FF, is a mixture of a pretreated biogas stream containing only CO_2 and CH_4 and renewable hydrogen from alkaline electrolysis of water and the composition in mol fraction, y, is presents in Table 1.

Table 1: Fresh Feed Composition in mol fraction for each component.

Mol fraction					
CO	CO_2	H_2	H_2O	CH_3OH	CH_4
0	0.248	0.750	0	0	0.002

The catalytic reactor feed composition is a mix of the fresh feed and the recycle gases and it is kept under stoichiometric proportions as it provides highest methanol yields and lowest recycle rations when compared to an excess of CO_2 or H_2 The stoichiometric number, SN, of the inlet can be calculated with Equation 4.(Ott *et al.*, 2012; Meyer *et al.*, 2016)

$$SN = \frac{y_{H_2} - y_{CO_2}}{y_{CO} + y_{CO_2}} \quad (4)$$

Typically, under industrial conditions, SN is between 2.01 and 2.1, implying a little excess of H_2, as it increases methanol selectivity due to hydrogen accumulation, leading to an optimum methanol synthesis.(Ott *et al.*, 2012)

3.1.3 Kinetics

Over the course of 45 years, many different authors have studied the kinetics of methanol synthesis, but, still, the is a lot of disagreement in the literature about which is the most reliable kinetic pathway, also most of them were developed in a type of Cu/ZnO catalyst. However, there are two kinetic models that are the most used ones, they are based on the experimental work of Graaf *et al.*(1990). and the one of Vanden Bussche and Froment(1996).

With regards on the kinetic model of Vanden Bussche and Froment(1996), the mechanism used is the Langmuir-Hinshelwood, they assumed that both hydrogen and carbon dioxide undergo dissociative adsorption on copper active sites and the rate determining steps is the hydrogenation of formate. This kinetic study revealed that Graaf *et al.*(1990) did not account for the fact that some intermediates like the formyl and methoxy species are predicted simultaneously in their model and present in two different reactions at the same time.

Based on the information above, the kinetic model chosen in this thesis will be the one of Vanden Bussche and Froment(1996), which is known to allow extrapolation outside of the experimental conditions, that are between the pressures of 15 and 51 bar and temperatures of 453 and 553 K. (Bozzano and Manenti, 2016)

Nevertheless, the model is based on reactions given by Equations 2 and 3, it assumes that the CO_2 is the main source of carbon for the synthesis of methanol and that there is negligible inhibition of the reaction in Equation 2. In addition, it considers the inhibitory effect of water formed by the RWGS reaction. The rate expressions for the two rate-determining steps, methanol synthesis and reverse water gas shift reaction are expressed in terms of partial pressure, p, by Equations 5 and 6, respectively.(Vanden Bussche and Froment, 1996)

$$r_{CH_3OH} = \frac{k_1\, p_{CO_2} p_{H_2} \left(1 - \frac{1}{K_{eq1}} \frac{p_{H_2O}\, p_{CH_3OH}}{p_{H_2}^3\, p_{CO_2}}\right)}{\left(1 + k_2 \frac{p_{H_2O}}{p_{H_2}} + k_3\, p_{H_2}^{0.5} + k_4\, p_{H_2O}\right)^3} \quad (5)$$

$$r_{RWGS} = \frac{k_5\, p_{CO_2}\left(1 - K_{eq2}\frac{p_{H_2O}\, p_{CO}}{p_{H_2}\, p_{CO_2}}\right)}{\left(1 + k_2\frac{p_{H_2O}}{p_{H_2}} + k_3\, p_{H_2}^{0.5} + k_4\, p_{H_2O}\right)} \quad (6)$$

The kinetic constants follow the Arrhenius law and it is expressed by Equation 7, also, its parameters, $\mathrm{A_k}$and $\mathrm{B_k}$, are shown in Table 2. The thermodynamic equilibrium constants are given by Graaf and Winkelman(2016) and calculated with Equations 8 and 9.

$$k_i = A_{ki}\, exp\left(\frac{\mathrm{B}_{ki}}{\mathrm{R_g}T}\right) \quad (7)$$

$$log_{10}(K_{eq1}) = \frac{3066}{T} - 10.592 \quad (8)$$

$$log_{10}\left(\frac{1}{K_{eq2}}\right) = -\frac{2073}{T} + 2.029 \quad (9)$$

Where T is the reaction temperature and $\mathrm{R_g}$ is the universal gas constant has a value of 8.314 J mol^{-1} K^{-1}.

Table 2: Kinetic parameters.

Kinetic constant	Kinetic parameters	
k_1 / mol kg^{-1} s^{-1} bar^{-2}	$\mathrm{A_{k1}}$	1.07
	$\mathrm{B_{k1}}$	36 696
k_2	$\mathrm{A_{k2}}$	3 453.38
	$\mathrm{B_{k2}}$	0
k_3 / bar$^{-1/2}$	$\mathrm{A_{k3}}$	0.499
	$\mathrm{B_{k3}}$	17 197
k_4 / bar^{-1}	$\mathrm{A_{k4}}$	6.62 10^{-11}
	$\mathrm{B_{k4}}$	124 119
k_5 / mol kg^{-1} s^{-1} bar^{-1}	$\mathrm{A_{k5}}$	1.22 10^{10}
	$\mathrm{B_{k5}}$	-94 765

3.1.4 Mathematical Model of the Reactor

Both of the catalytic reactors will be modeled as steady state multi-tubular fixed bed shell and tube reactor, in which the reaction occurs inside the tubes. The difference between

them is that one will be adiabatic and the second will be gas cooled with the recycle gases in the shell side.

The methanol synthesis reactor is commonly modeled as pseudo-homogeneous instead of heterogeneous because it requires less computational effort and yields similar results according to Rezaie et al. (2005). Also, it will be considered only axial direction, since the small diameter of the tubes and the high velocity of the gases make the radial dispersion negligible. No side reactions will be considered and the vestigial methane in the inlet stream will be considered as an inert in the process.

Additionally, in the model of Vanden Bussche and Froment(1996), there is no information whether the reaction kinetics have diffusional limitations, differently than the Graaf et al.(1990) that has it mentioned. Moreover, it was shown, in a comparative study between both kinetics, that the use of the Graaf et al.(1990) model with the diffusional limitations expressed as a function of effectiveness factor and the Vanden Bussche and Froment(1996) one without taking it into account generated remarkably similar results once the thermodynamic equilibrium was achieved under stoichiometric inlet conditions.(Meyer et al., 2016) Also, the catalyst considered is $Cu/ZnO/Al_2O_3$ and its characteristic can be found in Annex A.

3.1.4.1 Mass and Energy Balance and Pressure Drop

The mass balance is the same for both adiabatic and gas cooled reactors, Equation 10, and will be formulated in terms of mass fractions, ω, as it accounts for the decrease in the number of moles along the reactor.

$$\frac{M_T}{A_i}\frac{\mathrm{d}\omega_i}{\mathrm{d}z} = \rho_{\mathrm{cat}}(1-\varepsilon_{\mathrm{b}})\sum_{j}^{\mathrm{NR}} \nu_i MW_i r_j \tag{10}$$

Where ρ_{cat} is the density of the catalyst particle, MW is the molecular weight and ε_b is the bed voidage, their values can be found in Annex A, also NR is the number of reactions, M_T is the total mass flowrate inside the tubes, A_i is the transversal area of the tube, z is the axial reactor coordinate, and ν is the stoichiometric coefficient.

For the energy balance, Equation 11 and Equation 12 are the ones that refer to the tube side on the adiabatic and gas cooled reactor, respectively.

$$\frac{M_T\, Cp_g}{A_i}\frac{\mathrm{d}T_b}{\mathrm{d}z} = \rho_{cat}(1-\varepsilon_b)\sum_{j}^{NR} -\Delta H_j^r r_j \tag{11}$$

$$\frac{M_T\, Cp_g}{A_i}\frac{\mathrm{d}T_b}{\mathrm{d}z} = \rho_{cat}(1-\varepsilon_b)\sum_{j}^{\mathrm{NR}} -\Delta H_j^r r_j + \frac{\pi\, d_i}{A_i}\, U_{tube}\,(T_{shell}-T_b) \tag{12}$$

Where Cp_g is the heat capacity of the gas mixture and ΔH^r is the reaction enthalpy which are both defined in Annex A, T_b is the temperature of the bulk, U_{tube} is the overall heat transfer coefficient on the tube side, T_{shell} is the temperature on the shell side and d_i is the inner diameter of the tube.

Meanwhile, Equation 13 indicates the energy balance on the shell side in the gas cooled reactor.

$$\frac{M_T\ Cp_g}{A_i}\ \frac{dT_{shell}}{dz} = -\frac{\pi\ d_i}{A_i}\ U_{shell}\ (T_b - T_{shell}) \tag{13}$$

Where U_{shell} is the overall heat transfer coefficient on the shell side.

To determine the convective heat transfer coefficient for the shell side, $h_{o,R}$, the Churchill and Bernstein correlation is used, Equation 14, which is applicable for Reynold numbers, $\mathrm{Re_D}$, and Prandtl numbers, Pr higher than 0.2. (Perry *et al.*, 2000)

$$\frac{h_{o,R}\ D_h}{k_f} = 0.3 + \frac{0.62\ \mathrm{Re_D^{1/2}}\ \mathrm{Pr^{1/3}}}{\left[1 + \left(\frac{0.4}{\mathrm{Pr}}\right)^{2/3}\right]^{1/4}}\left[1 + \left(\frac{\mathrm{Re_D}}{282000}\right)^{5/8}\right]^{4/5} \tag{14}$$

The equations used to calculate the Reynolds number and the Prandtl number on the shell side are given by Equations 15, 16, respectively.(Sadik Kakaç, Hongtan Liu, 1998)

$$\mathrm{Re_D} = \frac{\rho_g v_o\ D_h}{\mu_g} \tag{15}$$

$$\mathrm{Pr} = \frac{Cp_g\ \mu_g}{k_f} \tag{16}$$

Where k_f is the thermal conductivity, ρ_g is the density and μ_g is the viscosity all of them referring to the gas mixture and their definitions can be found in Annex A.

Besides that, v_o is the velocity of the gas mixture inside the shell and it is defined by Equation 17, where D_s is the inside diameter of the shell, $\dot{m}_o$ is the mass flowrate inside the shell and N_t is the number of tubes.

$$v_o = \frac{\dot{m}_o}{\rho_g\left(\pi\ \frac{D_s^2}{4} - \pi\ N_t\ \frac{d_o^2}{4}\right)} \tag{17}$$

The diameter considered for the Equation 15 is the hydraulic diameter, D_h, and it is calculated based on the tube layout in Equation 18.

$$D_h = \frac{4\left(\frac{P_t^2\sqrt{3}}{4} - \frac{\pi d_0^2}{8}\right)}{\pi\, d_0/_2} \tag{18}$$

The convective heat transfer coefficient for the tube side in a packed bed, $h_{i,PB}$, is given by the Chilton-Colburn analogy in Equation 19.(Smith, 1981)

$$\frac{h_{i,PB}}{Cp_g\, M_T/_{A_i}}\left(\frac{Cp_g\,\mu_g}{k_f}\right)^{2/3} = \frac{0.458}{\varepsilon_b}\left(\frac{d_p\,\rho_g\,v_i}{\mu_g}\right)^{-0.407} \tag{19}$$

Where d_p is the diameter of the catalyst particle, found is Annex A, and v_i is the velocity of the gas mixture inside the tube expressed by Equation 20. Also, $\dot{m}_i$ is the mass flowrate inside one tube.(Sadik Kakaç, Hongtan Liu, 1998)

$$v_i = \frac{\dot{m}_i\, N_t}{\rho_g\left(\pi\,\frac{d_i^2}{4}\right)} \tag{20}$$

The overall heat transfer coefficient for the tube, and shell side are expressed by Equations 21 and 22, respectively.(Kern, 1950)

$$\frac{1}{U_{tube}} = \frac{1}{h_i} + \frac{d_i\,\ln d_o/d_i}{2\;k_w} + \frac{d_i}{d_o\,h_i} \tag{21}$$

$$\frac{1}{U_{shell}} = \frac{d_o}{d_i\,h_i} + \frac{d_o\,\ln d_o/d_i}{2\;k_w} + \frac{1}{h_o} \tag{22}$$

Where k_w is the thermal conductivity of the tube wall and it is defined in Annex A and h_i and h_o can be replaced for the respective tube and shell side convective heat transfer coefficients.

The initial pressure is considered 75 bar, but there is a pressure drop in the packed bed reactor and it is calculated with the Ergun's equation in Equation 23. (Ergun, 1952)

$$-\frac{dP}{dz} = \left(150\,\frac{(1-\varepsilon_b)}{Re_i} + 1.75\right)\frac{v_i^2\rho_g}{d_p}\,\frac{1-\varepsilon_b}{\varepsilon_b} \tag{23}$$

The Reynolds number inside the tube is given by Equation 24.

$$Re_i = \frac{\rho_g v_i\, d_i}{\mu_g} \tag{24}$$

3.1.5 Thermodynamic Framework

Considering the conditions under which the reactor operates, the nonideal behavior of the gases should be taken into consideration with the use of a equation of state, for instance, the modified Soave-Redlich-Kwong, SRK EOS, described for polar system containing water and methanol.(Soave, 1972; Mathias, 1983)

For pure substances, the original SRK EOS is described by Equation 25, where *V* is the specific volume.

$$P = \frac{\mathrm{R_g} T}{V - b} - \frac{a(T)}{V(V + b)} \tag{25}$$

Writing it in the cubic form results in the Equation 26 and Z is defined as the compressibility factor:

$$Z^3 - Z^2 + (A - B - B^2)\, Z - A\, B = 0 \tag{26}$$

Where A and B are reduced attractive and repulsive parameters of the EOS given by Equations 27 and 28, respectively.

$$A = \frac{a\, P}{\mathrm{R_g}^2\, T^2} \tag{27}$$

$$B = \frac{b\, P}{\mathrm{R_g}\, T} \tag{28}$$

The attractive and repulsive parameters of the EOS, a and b, are calculated by Equations 29 and 30, respectively, using critical temperatures, T_c, critical pressures, P_c, and acentric factors, w, present in Table 3. Additionally, since the system in case is a mixture, a and b become composition dependent and the calculations will be made using simple mixing rules. The binary interaction parameter, k_{ij}, is a fitting parameter for each existing binary mixture and can be found also in Table 4.(Van Bennekom *et al.*, 2012)

$$a = \sum_{i=1}^{\mathrm{NC}} \sum_{j=1}^{\mathrm{NC}} y_i y_j \sqrt{a_i\, a_j}\left(1 - k_{ij}\right) \tag{29}$$

$$b = \sum_{i=1}^{\mathrm{NC}} y_i b_i \tag{30}$$

Furthermore, a and b are also temperature dependent and for each component of the mixture a_i and b_i are calculated as shown in Equations 31 and 3.32.

$$a_i = 0.42747\, \frac{\mathrm{R_g}^2 T_{c,i}^2}{P_{c,i}}\, \alpha_i \tag{31}$$

$$b_i = 0.08664 \frac{\mathrm{R_g} T_{c,i}}{P_{c,i}} \tag{32}$$

The temperature dependent dimensionless parameter α_i is given by Equation 33 and it is expressed in terms of reduced temperature, T_R defined by Equation 34. Also, polarity parameter, p_f, is added to α_i as a correction for the presence of polar components.(Graboski and Daubert, 1979; Mathias, 1983)

$${\alpha_i}^{0.5} = 1 + m_i(1 - \sqrt{T_{R,i}}) - p_{f,i}\left(1 - T_{R,i}\right)\left(0.7 - T_{R,i}\right) \tag{33}$$

$$T_{R,i} = \frac{T}{T_{c,i}} \tag{34}$$

The parameter m_i was obtained by fitting Equation 33 to a set of pure hydrocarbon vapor pressure data resulting in Equation 35.(Graboski and Daubert, 1979)

$$m_i = 0.48508 + 1.55191 w_i - 0.15613\, {w_i}^2 \tag{35}$$

Table 3: Critical properties, acentric factors, and polarity correction factors for the components involved in methanol synthesis.(Van Bennekom *et al.*, 2012)

Parameter	CO	CO_2	H_2	H_2O	CH_3OH	CH_4
T_c / K	133	304	33.0	647	513	190
P_c / bar	35	73.8	12.9	221	80.9	46.0
w	0.066	0.239	-0.216	0.344	0.556	0.011
p_f	0	0	0	0.128	0.236	0

Table 4: Binary interaction parameters for the modified SRK equation of state.(Van Bennekom *et al.*, 2012)

Component	CO	CO_2	H_2	H_2O	CH_3OH	CH_4
CO	-	0.1164	-0.0007	-0.474	-0.3700	0.0204
CO_2	0.1164	-	0.1164	0.3000	0.1000	0.0956
H_2	-0.0007	0.1164	-	-0.745	-0.125	0.0010
H_2O	-0.4740	0.3000	-0.745	-	-0.075	0.0140
CH_3OH	-0.3700	0.1000	-0.1250	-0.0750	-	0.0460
CH_4	0.0204	0.0956	0.0010	0.0140	0.0460	-

3.2 Economizer Section

The economizer will be modeled in MATLAB as a single pass shell and tube heat exchanger with and without baffles. One of the goals of this section is to cool down the gases inside the tube to a temperature cold enough to enter the condenser while the vapor faction of the gas mixture is still one. Therefore, this temperature needs to be above the bubble point for the calculated composition, for that a temperature of 140 °C was chosen. The second goal is to heat up the gases coming from the condenser to a temperature similar to the one of the inlet of the catalytic reactor.

Normally, the heat exchangers are operated in the horizontal direction, but in the case of the LOGIC, it is vertical, however, the calculations will be made considering it in the horizontal orientation.

3.2.1 Constructional Design Parameters

The heat that must be transferred between cold and hot steams, Q, can be calculated by Equation 36:

$$Q = M_T \, Cp_g \, \Delta T = \dot{m}_o \, Cp_g \, \Delta T \tag{36}$$

And then, the heat transferred in the heat exchanger is expressed by Equation 37 using the mean logarithmic temperature difference, ΔT_{LMTD}, given by Equation 38. (Kern, 1950)

$$Q = A_0 \, U_{shell} \, \Delta T_{LMTD} \tag{37}$$

$$\Delta T_{LMTD} = \frac{(T_{h1} - T_{c2}) - (T_{h2} - T_{c1})}{ln\left(\frac{(T_{h1} - T_{c2})}{(T_{h2} - T_{c1})}\right)} \tag{38}$$

Where T_{h1} is the outlet temperature of the catalytic reactor, T_{h2} is the inlet temperature of the condenser, T_{c1} is the outlet temperature of the condenser and T_{c2} is the temperature at the outlet of the reactor in the shell side.

The outside area of the tube, A_0, considering the length of the economizer L_E is given by Equation 39.

$$A_0 = \pi \, d_0 \, N_t \, L_E \tag{39}$$

From that, it is possible to calculate the diameter of the shell using Equation 40 considering the main constructional parameters. (Sadik Kakaç, Hongtan Liu, 1998)

$$D_S = 0.637 \sqrt{\frac{0.87}{0.93}} \left(\pi \, d_o^2 \, N_t \, {P_R}^2\right) \tag{40}$$

Where P_R is the pitch ratio, defined by the ratio between the tube pitch and the outside diameter of the tube.

3.2.2 Tube Side Heat Transfer Coefficient and Pressure Drop

The convective heat transfer coefficient on the tube side for the economizer, $h_{i,E}$, is given by the Gnielinski correlation for transitional and fully developed turbulent flow with the Reynolds number between 3000 and $5\,10^6$, Equation 41. For an efficient transference of heat, it is advisable to keep the flow inside this range.(Schmidt, 2010)

$$\frac{h_{i,E}\, d_i}{k_f} = \frac{\left(f_i/8\right)\,(\mathrm{Re_i} - 1000)\,\mathrm{Pr}}{1 + 12.7\,\left(f_i/8\right)^{1/2}\,(\mathrm{Pr}^{2/3} - 1)} \tag{41}$$

The friction factor in the tube side, f_i, is expressed by Equation 42. Re_i and Pr are calculated with Equations 24 and 16, respectively.

$$f_i = \frac{1}{(1.82\,\ln(\mathrm{Re_i}) - 1.64)^2} \tag{42}$$

The pressure drop inside the economizer's tube, ΔP_i, is calculated by the Darcy-Weisbach equation, Equation 43.(Alarifi *et al.*, 2015)

$$\Delta P_i = 4\, f_i\, \frac{L_E}{d_i}\, \rho_g\, \frac{v_i^2}{2} \tag{43}$$

3.2.3 Shell Side Heat Transfer Coefficient Without Baffles

When the baffles are not used, the fluid flows along the direction of the tubes. In this case, the convective heat transfer on the shell side, $h_{o,S}$, is calculated by the Churchill and Bernstein correlation, Equation 14, substituting $h_{o,R}$ by $h_{o,S}$.(Churchill and Bernstein, 1977)

The Fanning factor, f_o, can be obtained for different regions of the flow through the Equations 44 and 45.(Schmidt, 2010)

$$f_{o,S} = [1.58\,\log(\mathrm{Re_D}) - 3.28]^{-2} \quad \text{for } 2300 < \mathrm{Re_D} < 10000 \tag{44}$$

$$f_{o,S} = 0.00128 + 0.1143\,\mathrm{Re_D}^{-0{,}311} \quad \text{for } \mathrm{Re_D} \geq 10000 \tag{45}$$

For these two cases above mentioned, the pressure drop on the shell side, $\Delta P_{o,S}$, is calculated by the Darcy-Weisbach equation, Equation 46.(Alarifi *et al.*, 2015)

$$\Delta P_{o,S} = 4\, f_o\, \frac{L_E}{D_h}\, \rho_o\, \frac{v_o^2}{2} \tag{46}$$

3.2.4 Single Segmental Baffles Design

In a real baffled shell and tube heat exchanger, only a fraction of the shell side flow actually passes across the tube bundle, because, in reality, up to 40% of the total flow passes through low flow resistance bypass areas. The possible flow streams inside the shell are shown in Figure 7 and they are designated by letters: tube to baffle leakage(Stream A), Crossflow(Stream B), Crossflow bypass(Stream C), shell-baffle leakage(Stream E) and tube pass partition bypass(Stream F).(Thome, 2016)

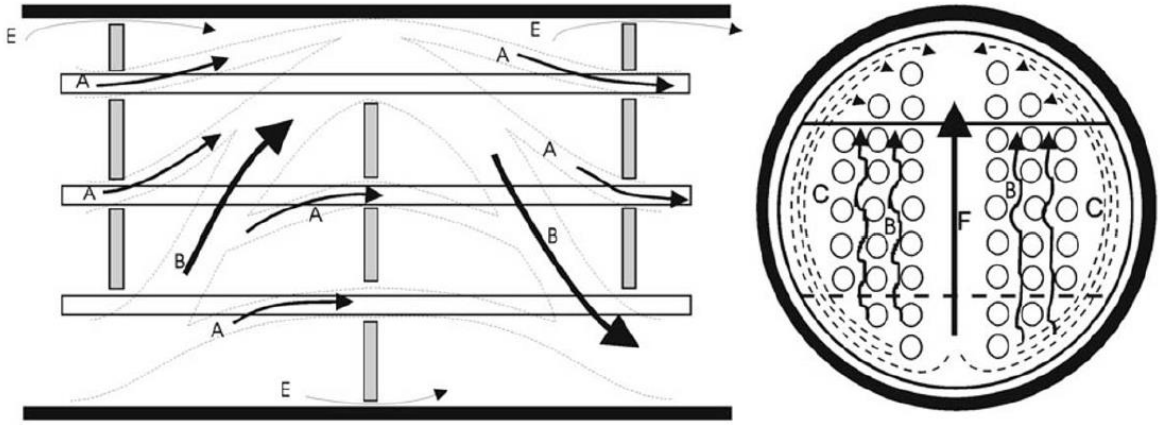

Figure 7: Flow model for the shell side of the heat exchanger.(Serna and Jiménez, 2005)

However, the full design of a baffled heat exchanger, considering all the possible losses, must be personalized for each case considering characteristics of the flow and the shell and tube dimensions. Therefore, this work will be based on the ideal case without contemplating any losses.

Nonetheless, one design parameter must be decided, the baffle spacing. It cannot be too short, because it causes poor penetration of the fluid across the tube bundle. However, it cannot be too large, or the fluid will be flowing mostly along the direction of tubes, minimizing the crossflow and, consequently, the heat transfer. The baffles also work as a support, so the tubes stay in place and avoids flow induced vibrations in the tubes. The TEMA standards (2007) recommends a baffle spacing between 30% and 60% the inner shell diameter. For this work the value chosen of baffle spacing, B_s, is 50% of the inside shell diameter.

Furthermore, because of this change, some other parameters must be redefined in relation to the ones previously mentioned.

Considering that the gases flow across the tube bundles, the minimum flow area in one baffle space at the center of the tube bundle, A_s, is given by Equation 47.(Thome, 2016)

$$A_s = \left(D_s - \frac{D_s}{P_t}\, d_o\right) B_s \tag{47}$$

From that, the Reynolds number, $\mathrm{Re_B}$, is calculated with Equation 48.

$$\mathrm{Re_B} = \frac{d_o\, \dot{m}_o}{\mu_g\, A_s} \tag{48}$$

3.2.5 Baffle Design

The Bell-Delaware method by Taborek (1983) will be used to determine the shell side heat transfer coefficient using single segmental baffles.

Without any of the losses mentioned, the ideal heat transfer coefficient for pure cross flow, $h_{o,B}$, is given by Equation 49.

$$h_{o,B} = j_i\, Cp_g \frac{\dot{m}_o}{A_s}\, \mathrm{Pr}^{-2/3} \tag{49}$$

Where the Colburn j-factor for an ideal tube bank, j_i, is defined by equation 50 and the empirical factor a is calculated with Equation 51.

$$j_i = a_1 \left(\frac{1.33}{P_t/d_o}\right)^a (\mathrm{Re_B})^{a_2} \tag{50}$$

$$a = \frac{a_3}{1 + 0.14\, (\mathrm{Re}_B)^{a_4}} \tag{51}$$

The friction factor for ideal tube bank, $f_{o,B}$, is calculated with Equation 52 and the empirical factor b is calculated with Equation 53.

$$f_{o,B} = b_1 \left(\frac{1.33}{P_t/d_o}\right)^b (\mathrm{Re_B})^{b_2} \tag{52}$$

$$b = \frac{b_3}{1 + 0.14\, (\mathrm{Re_B})^{b_4}} \tag{53}$$

Where a1, a2, a3, a4, b1, b2, b3 and b4 are correlational constants listed in Table 5 for the 30° tube layout angle.

Table 5: Empirical coefficients for calculation of j_i and f_i. (Taborek,1983)

Re_B	a_1	a_2	a_3	a_4	b_1	b_2	b_3	b_4
10^5-10^4	0.321	-0.388	1.45	0.519	0.372	-0.123	7.00	0.500
10^4-10^3	0.321	-0.388	—	—	0.486	-0.152	—	—
10^3-10^2	0.593	-0.477	—	—	4.57	-0.476	—	—
10^2-10	1.36	-0.657	—	—	45.1	-0.973	—	—
<10	1.40	-0.667	—	—	48.0	-1.00	—	—

From that, the ideal bundle pressure drop, $\Delta P_{o,B}$, is given by Equation 54.

$$\Delta P_{o,B} = 0.002\, f_o\, N_t\, \frac{\left(\dot{m}_o/A_s\right)^2}{\rho_g} \tag{54}$$

3.2.6 Overall Heat Transfer Coefficient

After calculating the convective heat transfer coefficients for the tube side and for both baffled and unbaffled shell side, Equation 22 is used to calculate the overall heat transfer coefficient, U_E, substituting h_o and h_i with the respective tube shell side convective heat transfer coefficients, $h_{i,E}$, $h_{o,S}$ and $h_{o,B}$.

Finally, the length of both economizers can be calculated with Equation 37.

3.3 Condenser Section

The condenser section will not be designed, because the dimensions must be personalized for each case considering characteristics of the flow and operational conditions. However, it will be simulated using the Flash Vessel in Aspen Plus with two outlets, one for the vapor stream and other for the liquid stream. Firstly, the inlet of this section has a temperature of 140 °C, in concordance with the previous section, but for the reactor to operate in natural convection, a temperature difference of around 70 °C is needed to generate the required density gradient (M.J. Bos and D.W.F. Brilman, 2015). Therefore, a flash temperature of 68 °C will be used and according to the vapor–liquid equilibrium diagram, VLE, of methanol and water mixture, this temperature is below the bubble point. (Perry *et al.*, 2000)

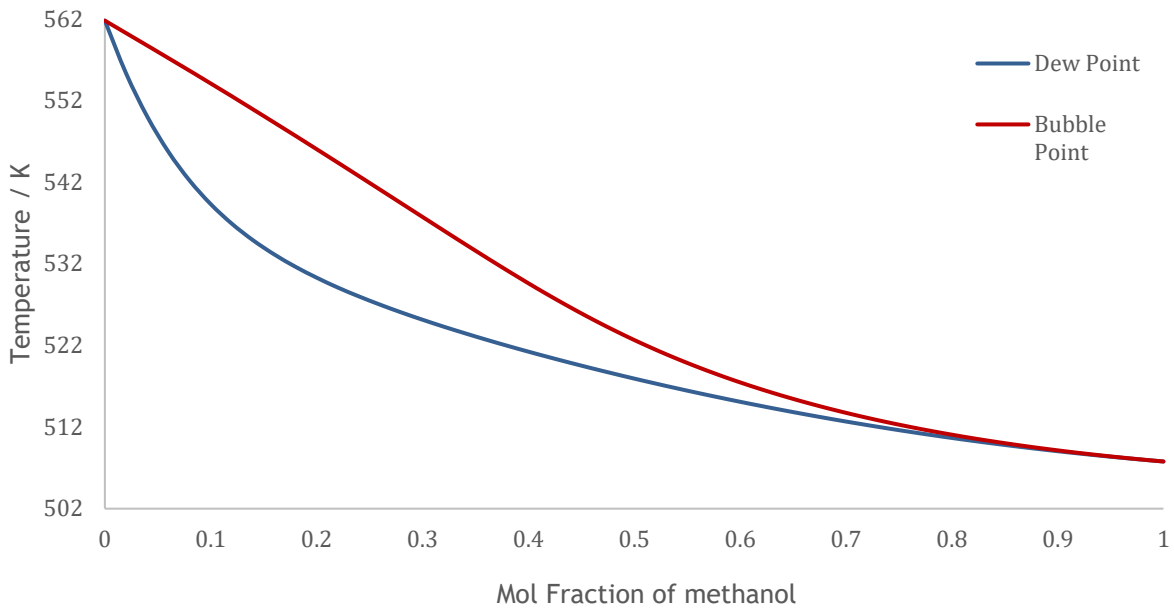

Figure 8: VLE diagram of methanol and water mixture for a constant pressure of 75 bar.

3.4 How the Program Works

To create the full Logic reactor, MATLAB and Aspen Plus are used together to generate the results, the scheme in Figure 9 exemplifies how it works.

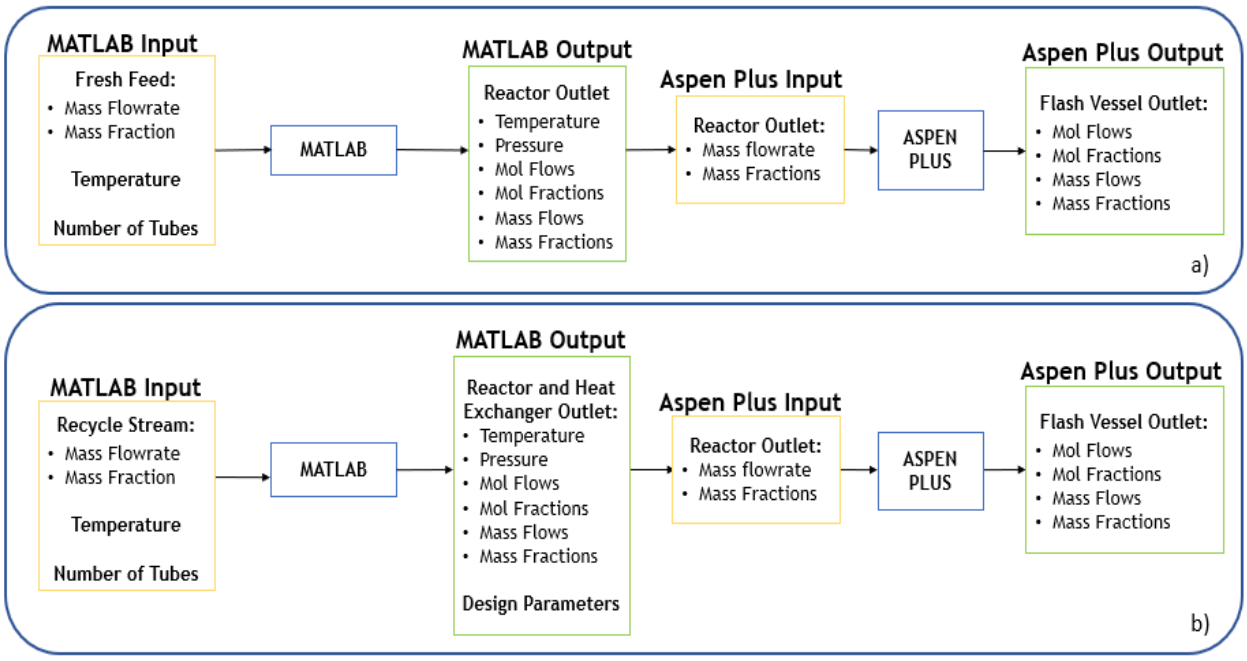

Figure 9: Scheme of the LOGIC reactor algorithm: a) Recycle stream estimative and b) Result generation.

The Logic reactor works with fluid circulating inside both a shell and tube, but at first the data of the fluid in the shell is unknown, because of that, the first block in Figure 9a) is used to generate this estimative. First, MATLAB is used to run only the catalytic reactor code with fresh feed as the full inlet stream, requiring the data of the mass flowrate, mass fraction, inlet temperature and the number of tubes. From the output of MATLAB, only the mass flowrate and the mass fraction are used as input for the Aspen Plus program that generates the liquid and vapor streams, being the last one the estimation for shell side gas stream.

The second block, in Figure 9b), works similarly to the first one with only two differences. The input data introduced in the MATLAB program is the recycle stream data, as the program calculates the mixed inlet of the reactor and the output is the same as the first plus the design parameters of the reactor and heat exchanger.

The MATLAB codes developed are available in Appendix A.

4 Results and Discussion

To determine the best design for the LOGIC reactor, a comparative analysis was made changing four parameters as demonstrated in Table 6 with their respective values.

Table 6: Varied parameters for the comparative analysis.

Varied Parameters			
Inlet Temperature / K	**Number of Tubes**	**Reactor Type**	**Economizer Type**
513	2000	Adiabatic	Baffled
523	1500		
533	1000	Gas Cooled	Unbaffled
543	500		

In this chapter, it will be discussed how these variables affect the main design parameters of the catalytic reactor and the economizer. In Table 7, there is a summary of the data already mentioned in the previous chapter that will be kept constant.

Table 7: Summary of the fixed parameters.

Fixed Parameters		
d_i / m	0.0254	
d_o / m	0.0349	
Condenser Temperature / K	341.15	
Condenser Inlet Temperature / K	413.15	
P_{in} / bar	75	
Tube layout	Triangular 30°	
Baffle Type	Single Segmental	
Tube pitch ratio	1.25	
Baffle spacing / m	0.5 D_S	
Mol fraction of the Fresh Feed	CO	0
	CO_2	0.248
	H_2	0.750
	H_2O	0
	CH_3OH	0
	CH_4	0.002

4.1 Catalytic Reactor

For this section, the varied parameters considered were the inlet temperature, the number of tubes and the catalytic reactor type. In Table 8, a "X" is used to indicate the dependency between observed and varied parameters.

Table 8: Dependency relation between varied and observed parameters in the catalytic section.

Observed Design Parameters	**Varied Parameters**		
	Inlet Temperature / K	Number of tubes	Reactor Type
Inlet Mass Flowrate / kg s^{-1}	X		
FF Mass Flowrate / kg s^{-1}			
Outlet Temperature / K	X		X
Recycle Ratio	X		X
Conversion / %	X		X
Gas Composition Profile			X
Reactor Length / m	X	X	
Catalyst Weight / kg	X	X	
Reynolds Number	X	X	
Overall Heat Transfer Coefficient / W m^{-2} K^{-1}	X	X	
Pressure Drop / Pa	X	X	

4.1.1 Inlet Mass Flowrate

Some considerations were made to promote a better visualization over this comparative study. The first is that the inlet mass flowrate of the catalytic reactor was varied in a way to keep the liquid methanol production constant at 525 kg h^{-1} for all the inlet temperatures, T_{in}, in the adiabatic reactor. From that, it was possible to observe how the methanol production and the fresh feed mass flowrate changes between the reactor types for the same inlet mass flowrate and temperature, as seen in Table 9.

Table 9: Mass flowrates and methanol production in the GCR for the different inlet temperatures while keeping the production of the AR constant.

	Inlet Temperature / K	**513**	**523**	**533**	**543**
	Total inlet mass flow / kg s^{-1}	1.63	1.79	1.97	2.2
	Fresh feed mass flow / kg s^{-1}	0.271	0.279	0.288	0.300
Liquid Methanol Production / kg h^{-1}	Adiabatic Reactor	525			
	Gas Cooled Reactor	586	570	560	552

From Table 9, it is possible to observe that increasing the inlet temperature, it is necessary a higher total inlet and fresh feed mass flowrate to keep the methanol production constant in the adiabatic reactor. Also, it is possible to note that the methanol production increased when the GCR was used.

Also, the stoichiometric number of the total inlet mass flowrate of the catalytic reactor presented values between 2.02 and 2.03, as it can be seen in Appendix B, being inside the optimal range defined in section 3.1.2.

4.1.2 Outlet Temperature and Recycle Ratio

To have a better understanding of the temperature profile inside the reactor, another consideration must be made, it consists in keeping the length constant for both reactor types. It was calculated as the necessary length for the adiabatic reactor to reach thermodynamic equilibrium. Figure 10 is an example of the temperature profile inside for both reactors with 1500 tube for an inlet temperature of 533.15 K.

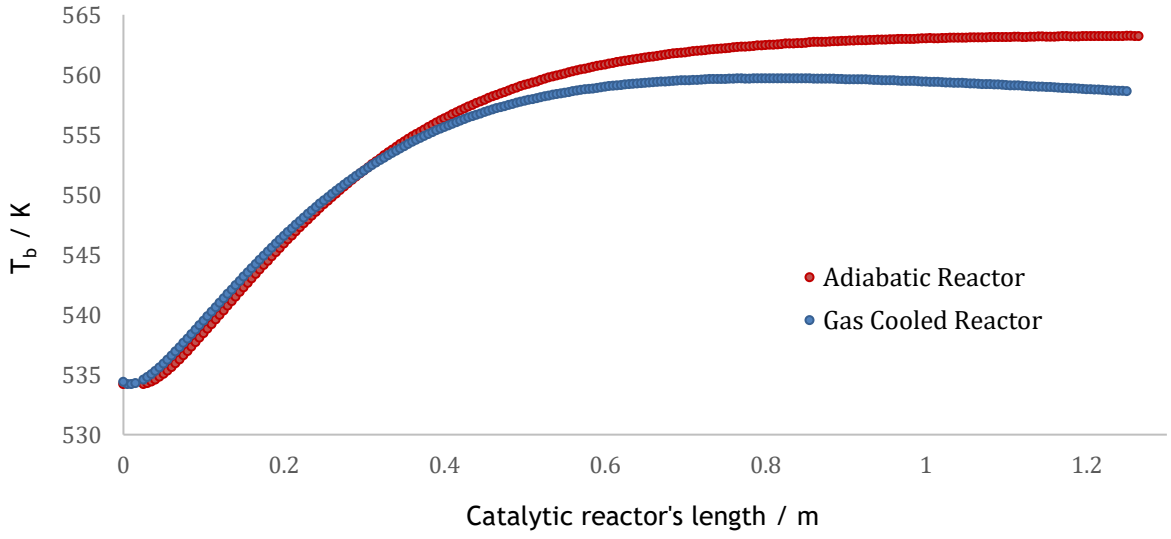

Figure 10: Temperature profile for both reactors with 1500 tube for an inlet temperature of 533.15 K.

As it can be observed, in the GCR, instead of the temperature stabilizing, it decreases, due to heat transfer with the gases in the shell side. In Figure 11, it is possible to see how the outlet temperature changes as a function of the inlet temperature.

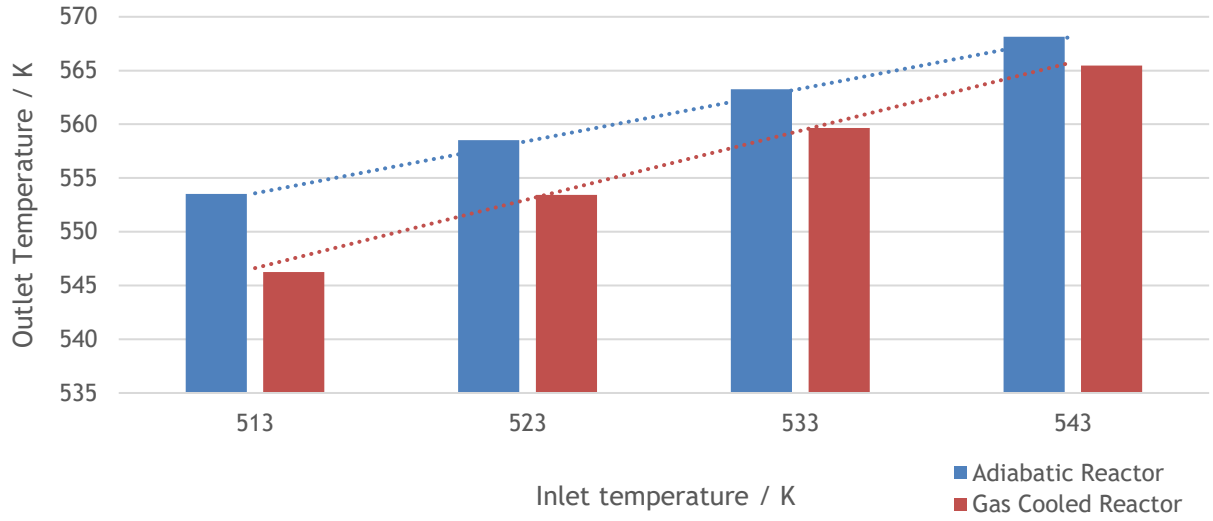

Figure 11: Outlet temperature variation as a function of the inlet temperature for both reactors with 1500 tubes.

It was to expect, as the overall synthesis reaction is exothermic, that, the higher the inlet temperature, the higher the outlet one would be. Besides that, as shown in Figure 12, the difference between them decreases as the inlet temperature increases. This effect is due to the kinetics being favored when in higher temperatures, making the reaction occur faster.

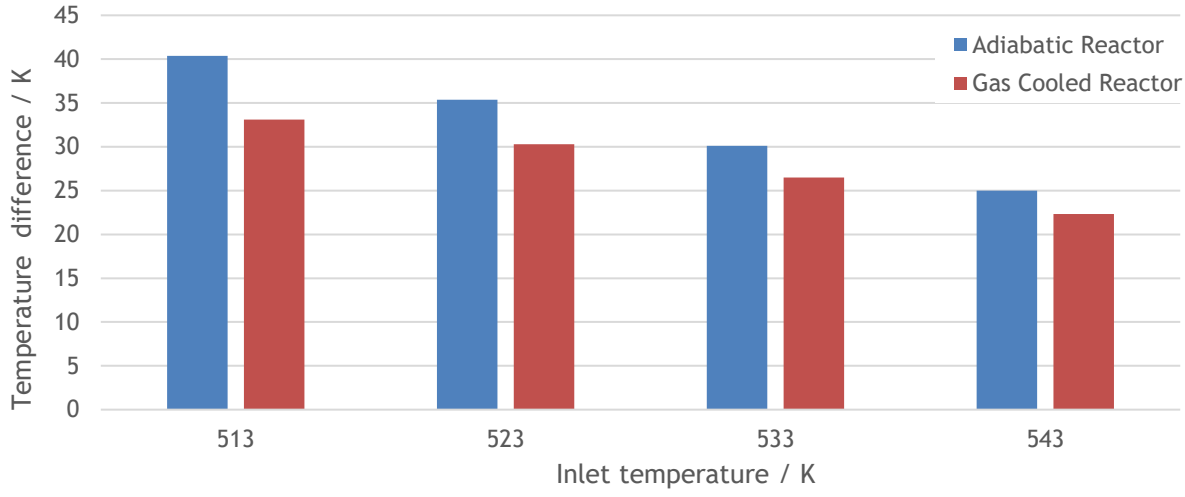

Figure 12: Variation of the temperature difference between inlet and outlet temperatures as a function of the inlet temperature for both reactors with 1500 tubes.

In Figure 11, it is possible to verify a linear relation between the outlet and the inlet temperatures on both reactors, described by Equation 55 and 56.

$$T_{out}^{AR} = 4.859\, T_{in} + 548.72 \tag{55}$$

$$T_{out}^{GCR} = 6.387\, T_{in} + 540.23 \quad (56)$$

The coefficient of determination, R^2, for the linear equations of the adiabatic reactor and the gas cooled reactor were 0.9999 and 0.9976, respectively, indicating a high linearity on both cases. This may be caused by the assumptions made in section 3.1.4, considering the reactor to be pseudo homogeneous without diffusional limitations, also the small range of operational conditions studied contributes for the linear behavior to happen. Besides that, the fact that the R^2 for the GCR is lower can be attributed to the term of heat exchange present in the energy balance in Equation 12.

Although the lowest inlet temperatures and the use of GCR cause the recycle ratio to be smaller, due to higher conversions, the values do not vary a lot among the cases studied, as seen in Table 10, the mean of all the values in it is 0.85 ± 0.0002. This factor also contributes to this linear behavior observed.

Table 10: Recycle ration of both reactors varying with the inlet temperature.

T_{in} / K	Recycle Ratio	
	Adiabatic Reactor	Gas Cooled Reactor
543	0.867	0.863
533	0.857	0.852
523	0.847	0.839
513	0.836	0.824

4.1.3 Conversion

As mentioned previously, the conversion of the overall methanol synthesis is lower at higher temperatures due to thermodynamic limitations and this behavior can be validated as shown in Figure 13.

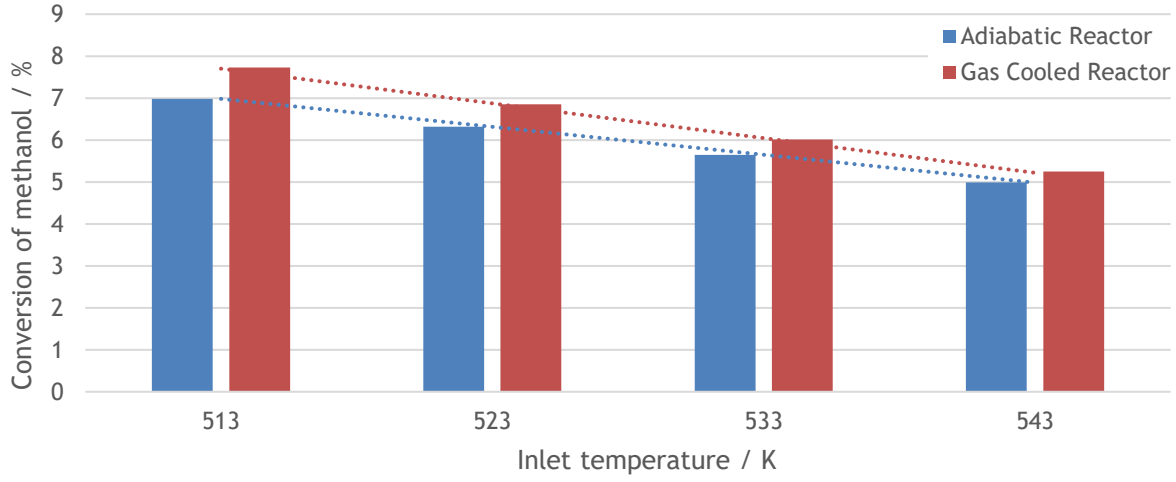

Figure 13: Conversion of the overall methanol synthesis as a function of the inlet temperature for both reactors.

The increase of the inlet temperature does lower the conversion, but also it is possible to verify that the GCR even promotes a bigger one, because, as seen in Figure 11, the overall temperature in this reactor is smaller. This confirms that an efficient temperature control is essential to have a high methanol conversion.

Furthermore, this study also presents a linear behavior, described by Equation 57 and 58, with a coefficient of determination for the adiabatic reactor and the gas cooled reactor being 1 and 0.999, respectively, indicating an even higher linearity on both cases.

$$Conversion_{AR} = -0.666\, T_{in} + 7.643 \quad (57)$$

$$Conversion_{GCR} = -0.827\, T_{in} + 8.528 \quad (58)$$

4.1.4 Gas Composition Profile

The main difference between AR and GCR lays on the fact that the second presents overall lower temperatures along the reactor, which affects the equilibrium of the reactions involved in the methanol synthesis. Therefore, this section will demonstrate the importance of temperature control to overcome the thermodynamic limitations in order to improve methanol production. For that, this study will be performed comparing outlet composition, in mass fraction, of both reactors at an inlet temperature of 533.15 K and 1500 tubes.

Taking into consideration the reactions involved in this process, the hydrogenation of CO_2, Equation 2, and the reverse water gas shift, Equation 3, the first is exothermic, meaning the decrease in temperature favors product formation. However, the RWGS reaction is endothermic, so low temperatures shift the equilibrium to the reactant production.

First, considering the reactants' profiles presented in Figure 14, as the equilibrium of the RWGS is shifted away from the product side, more CO_2 and H_2 are formed and consumed in the methanol synthesis reaction.

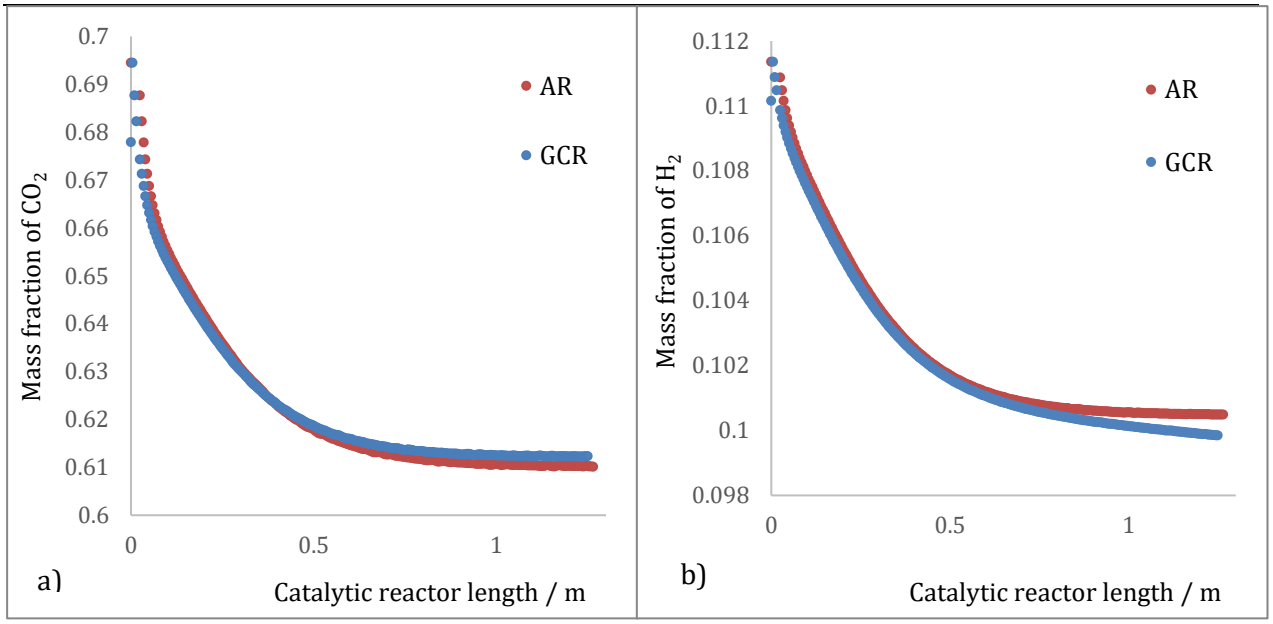

Figure 14: Composition profile along the reactor for a) CO_2 and b) H_2.

However, at the end of the reactor the composition of CO_2 is higher and the one of H_2 is lower in the GCR, this happens because, as seen in equation 2, the CO_2 to H_2 proportion is 1:3, meaning more H_2 is consumed.

Regarding the profile of the CO, Figure 15, its outlet composition is lower in the GCR, because this component is only produced in the RWGS and the low temperatures in this reactor decrease its production.

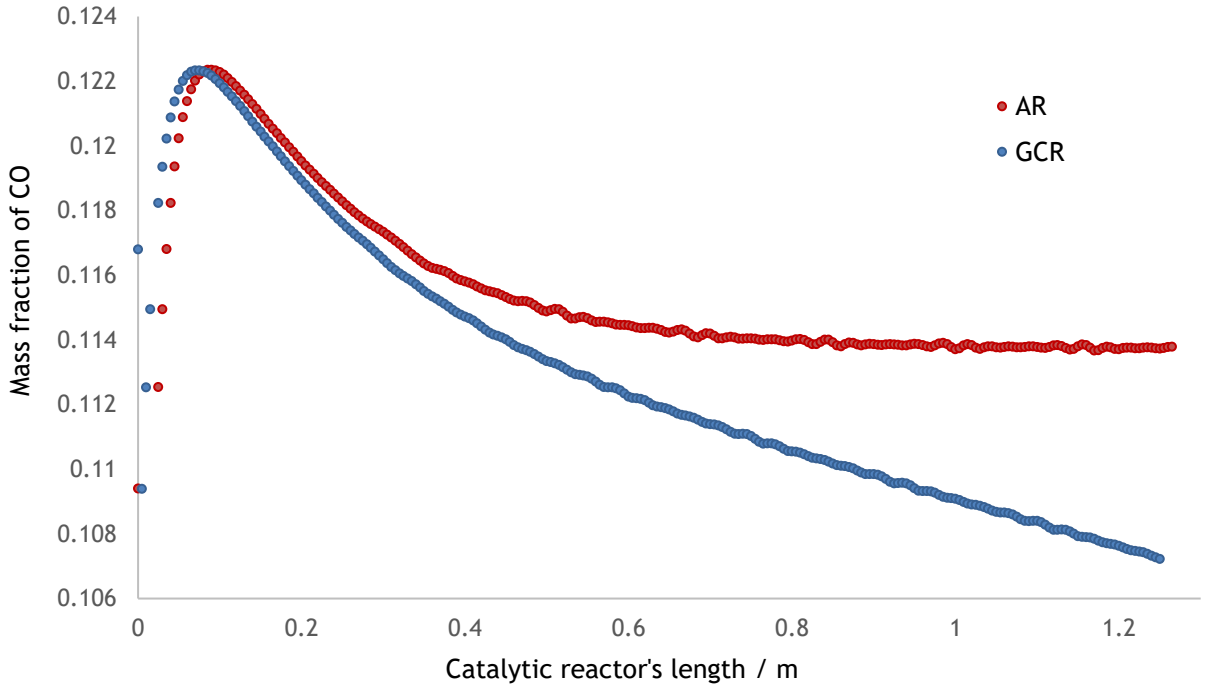

Figure 15: CO composition profile along the reactor.

Now, for the products, methanol and water, in Figure 16 it can be noted that the methanol composition in the GCR is higher, as already discussed. However, regarding the H_2O profile in the GCR, it is smaller due also to the equilibrium limitations of the RWGS, as already discussed.

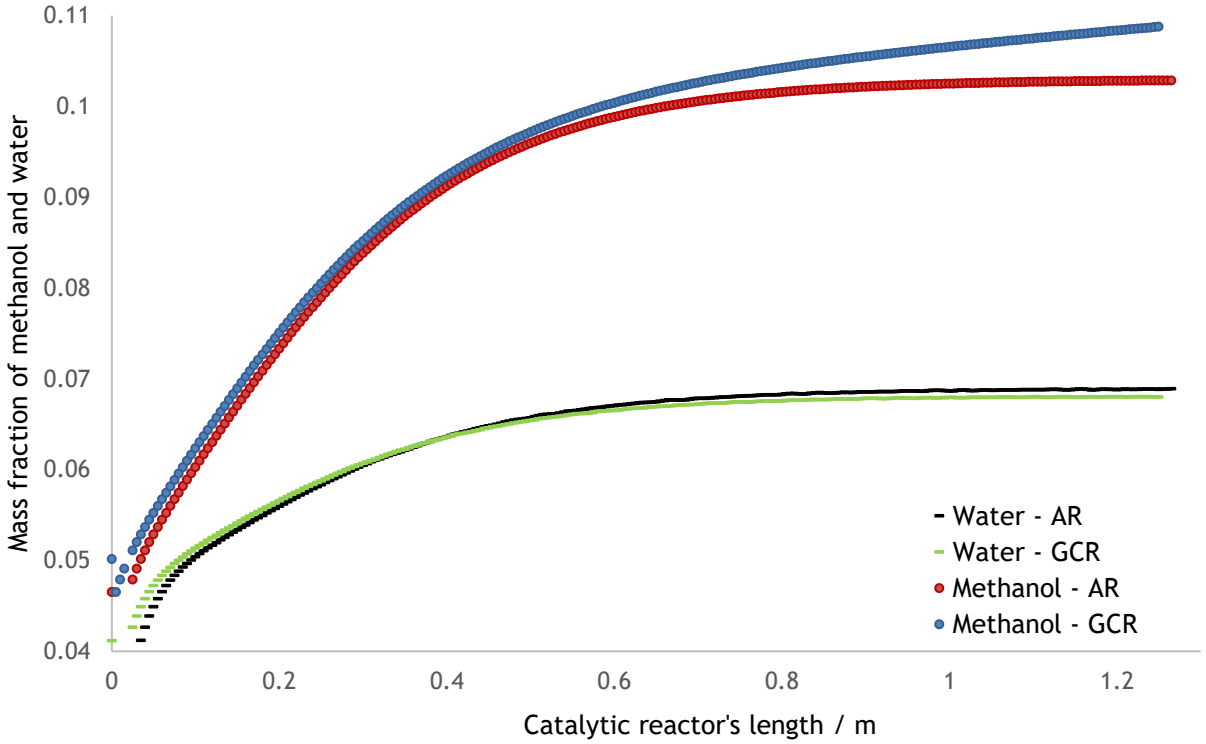

Figure 16: Methanol and Water composition profile along the reactor.

4.1.5 Reactor Length and Catalyst Weight

As mentioned before, the length of both reactor types was kept the same, but it still varies when submitted to a change in the number of tubes and inlet temperature, as seen in Figure 17.

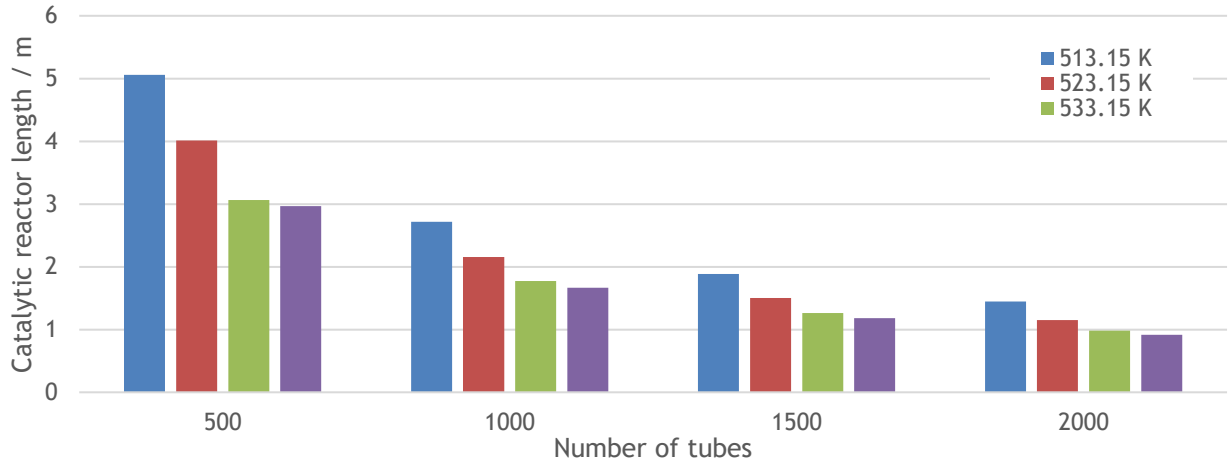

Figure 17: Adiabatic reactor's length variation with different tube amounts and inlet temperatures.

The length decreases as the temperature increases, because of the improved kinetics at higher temperatures and, as the number of tubes increase, there is no need for them to be as long for the reaction to be complete.

In Figure 18, the same behavior can be seen analyzing the catalyst weight load, calculated in Annex A, necessary for each case mentioned above.

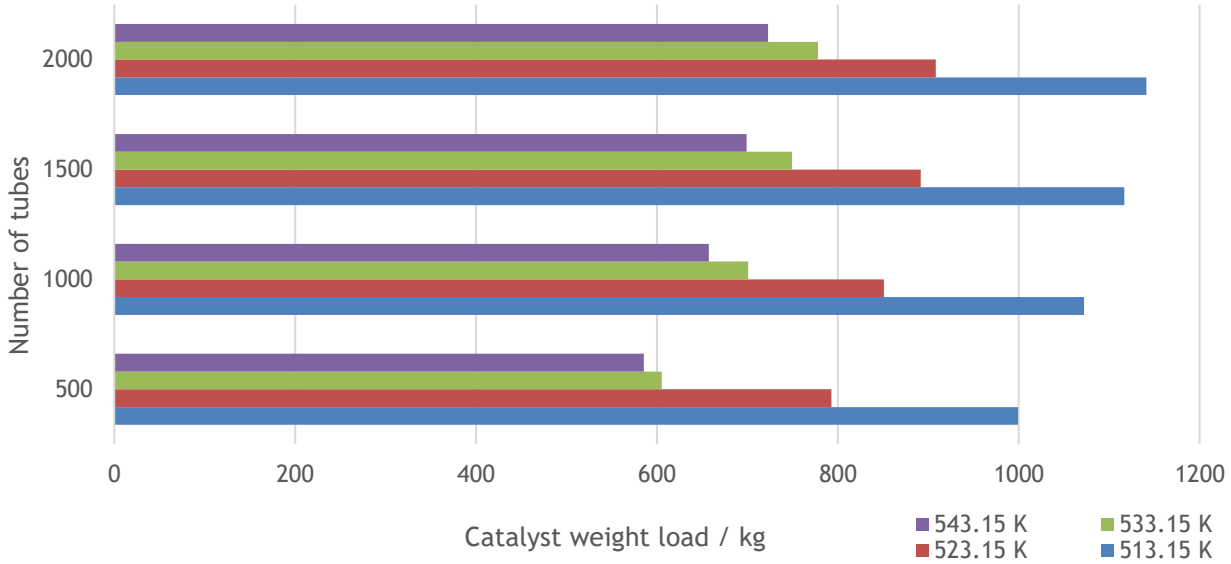

Figure 18: Catalyst weight load variation with different tube amounts and inlet temperatures.

Even though at lower temperatures the production is higher, it needs longer tubes and higher amounts of catalyst weight.

4.1.6 Reynolds Number and Overall Heat Transfer Coefficient

Now considering the flow inside the tube and the overall heat transfer coefficient, the study of these parameters will be done considering only the change in the inlet temperature and number of tubes.

As for the Re, the maximum difference of the values considering the two reactors is around $0.82\,\% \pm 0.50$, as it can be seen in Appendix B, therefore it will be only considered the results of the GCR in this section, so it can relate with the heat transfer coefficient analysis.

First, in Figure 19, it is possible to observe how the Reynolds number vary with the parameters considered. The Re increases when higher temperatures are used mainly because of the difference in flowrates, as shown in Table 9. Therefore, as the dimeter of the tubes are always constant, high flowrates leads to high Reynolds numbers.

Considering the variation regarding the number of tubes, it is much more pronounced. When the amount of tubes increases, the flow is divided inside the tubes, decreasing the velocity and, therefore, the Re.

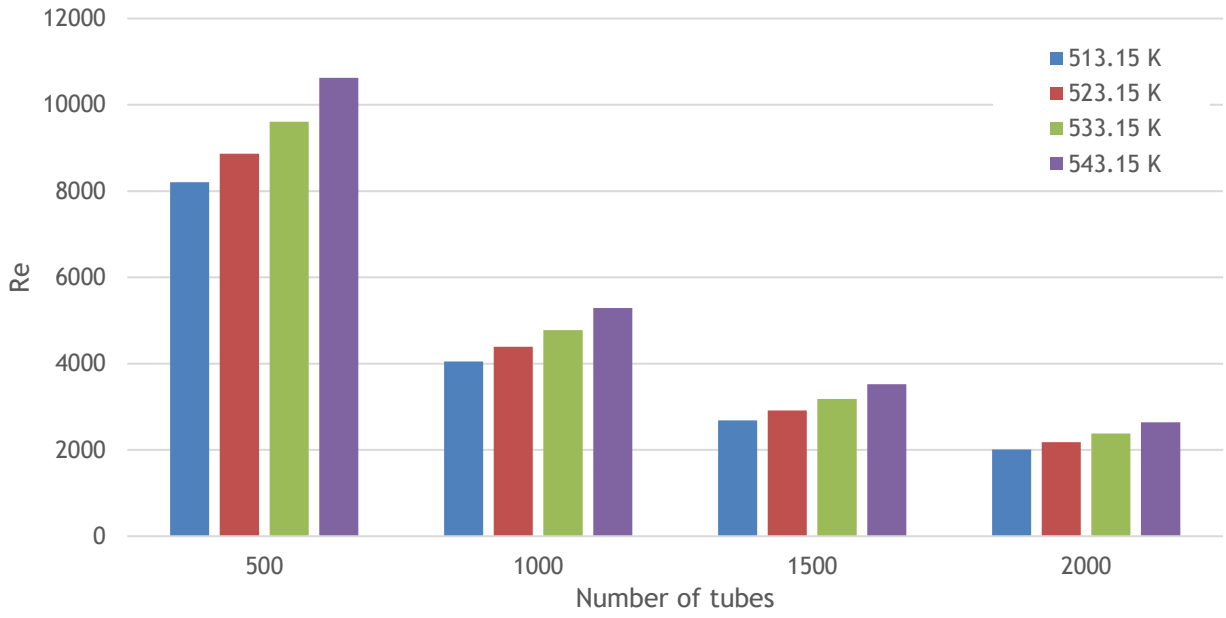

Figure 19: Tube side Re of the GCR varying with the inlet temperature and the number of tubes.

Figure 20 shows the behavior of the overall heat transfer coefficient of the GCR and it follows the same behavior of the Reynolds number. It is plausible because the increase in turbulence causes the heat exchange to be more efficient.

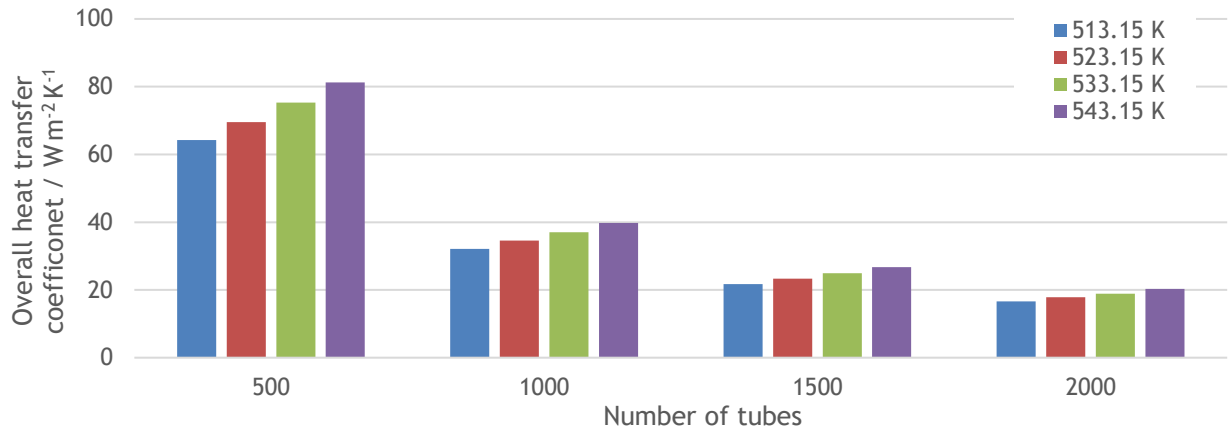

Figure 20: Overall heat transfer coefficient of the GCR varying with the inlet temperature and the number of tubes.

4.1.7 Pressure Drop

For the pressure drop analysis, the mean difference between the values considering the two reactors is around $1.12\,\% \pm 0.27$, as shown in Appendix B, being the GCR the one with the slightly higher values, so only the adiabatic reactor will be considered.

While evaluating the data in Figure 21, the values that stand out are the ones for the reactor with 500 tubes, this behavior can be explained considering the velocity inside the tubes. As mentioned above, the Re, when the reaction occurs inside 500 tubes, is the highest observed and characterizes turbulent regime, which causes high pressure drops.

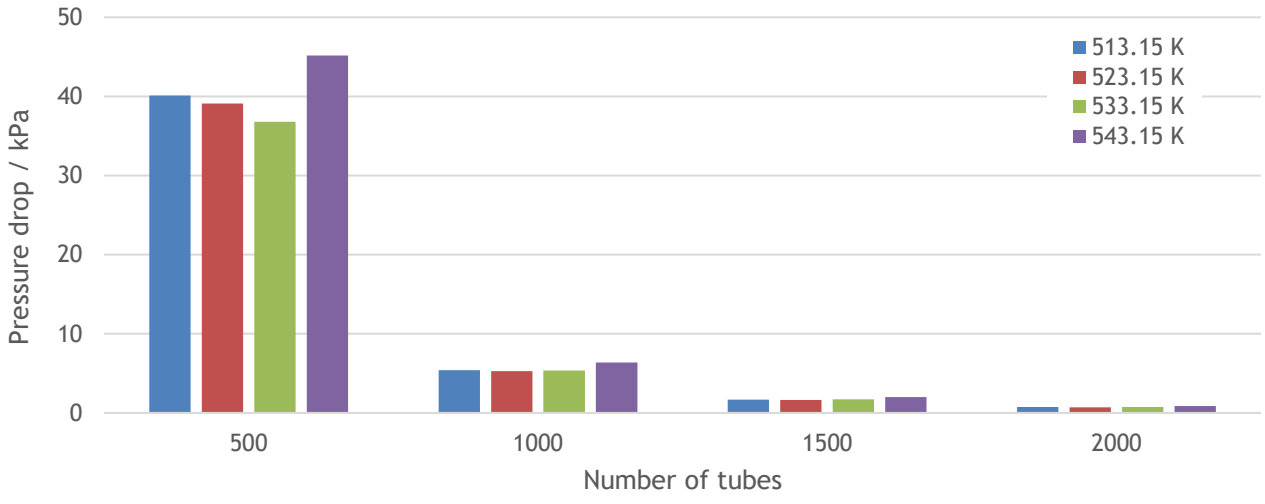

Figure 21: Tube side pressure drop of the AR varying with the inlet temperature and the number of tubes.

4.2 Economizer

This section will follow the same structure as the last and the varied parameters will be the same, but adding the presence of baffles, with a purpose of analyzing how they improve heat transfer. In Table 11, it is possible to see which of these will be considered to affect the main design parameters of the economizer when marked with a "X".

Table 11: Relation between varied and observed parameters in the catalytic section.

Observed Design Parameters	**Varied Parameters**			
	Inlet Temperature / K	Number of tubes	Reactor Type	Presence of Baffles
Economizer Length / m	X		X	X
Reynolds Number	X	X		X
Overall Heat Transfer Coefficient / $W\,m^{-2}\,K^{-1}$	X	X		X
Pressure Drop / Pa	X	X		X
L_t/D_s	X	X	X	X

4.2.1 Reynolds Number and Overall Heat Transfer Coefficient

The analysis of the Reynolds number is crucial as it characterizes the behavior of the flow. The presence of baffles will be studied over the different inlet temperatures and tube amount. Also, the mean difference between the values for the Re considering the two reactors is $0.95\,\% \pm 0.55$, as it can be seen in Appendix B, so only the results concerning the adiabatic reactor will be considered.

First, keeping the inlet temperature at $513.15\,K$, it is possible to understand the impact of the quantity of tubes, as shown in Figure 22.

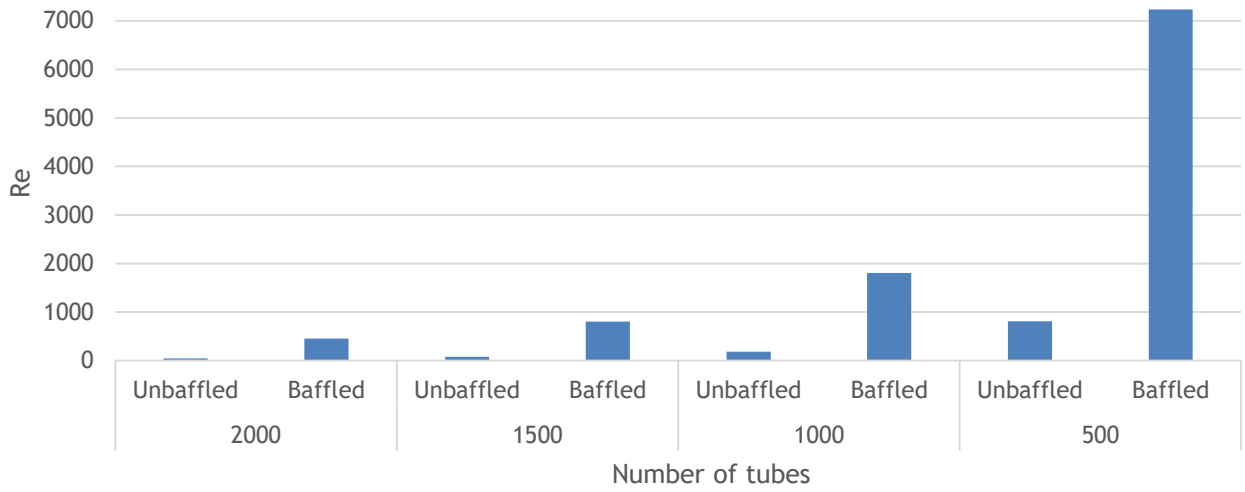

Figure 22: Shell side Re varying with the number of tubes for the baffled and unbaffled economizer at 513.15 K.

The presence of baffles increased the Reynolds number in around 900 %, but, besides that, this parameter grows considerably when the number of tubes is decreased, specially at 500 tubes. This happens because the minimum bundle cross flow area decreases together with the number of tubes, as it can be seen in Table 12. When this area is low, it creates difficulty for the gases to flow, leading to more turbulence and increasing the Re.

Table 12: Minimum bundle cross flow area for the different shell diameters and number of tubes.

N_t	2000	1500	1000	500
D_s / m	7.37	5.53	3.68	1.84
A_s / m²	0.023	0.019	0.013	0.006

Now taking into consideration the variation of the inlet temperature in a reactor with 1000 tubes, Figure 23 is used to represent the results.

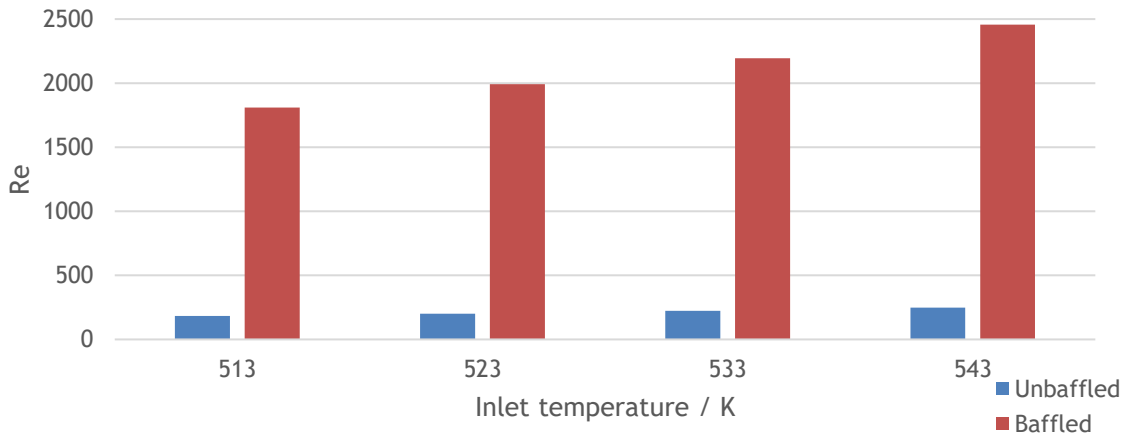

Figure 23: Shell side Re varying with the inlet temperature for the baffled and unbaffled economizer with 1000 tubes.

Again, the reactor with baffles presents much higher Re, but besides that it increases with temperature as it happened in Section 4.1.6 due to the inlet mass flowrates.

As already stated in Section 4.1.6, the behavior of the overall heat transfer coefficient follows the same pattern as the Reynolds number. As it can be seen in Figure 24, the heat transfer is increased when the baffles are used in overall 140 %, considering the variation in number of tubes.

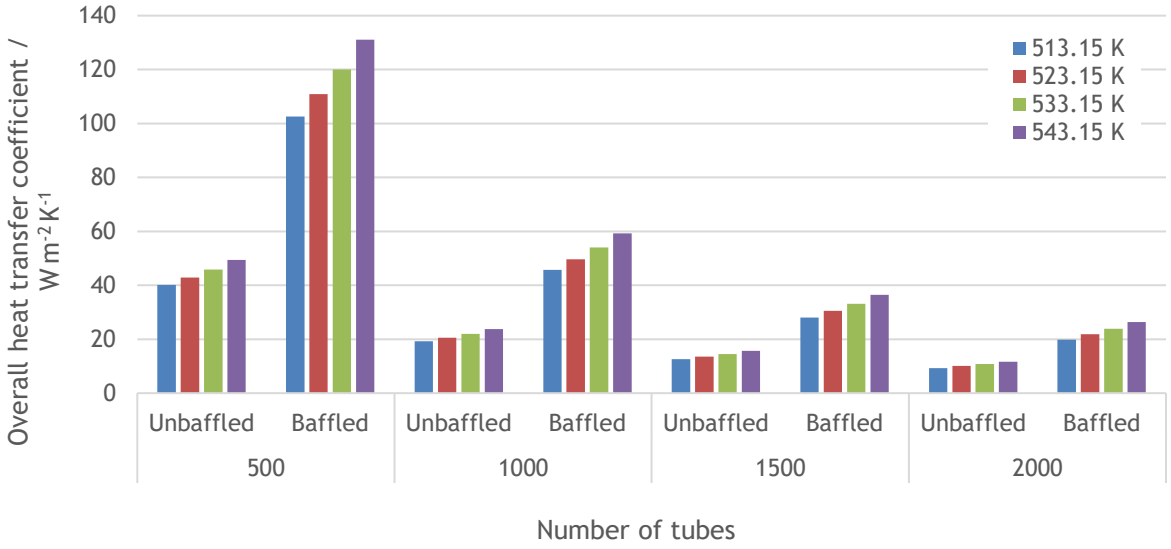

Figure 24: The overall heat transfer coefficient varying with the inlet temperature and the number of tubes in a baffled and unbaffled economizer.

4.2.2 Length of Economizer

The length of the economizer decreases when the number of tubes is lower, also this difference is higher when the baffles are present, due to improved heat exchange. However, the overall difference is considerably low, as it can be seen in Appendix B, so the following analysis will be made taking into consideration only the inlet temperature and both reactors with 1000 tubes.

The use of baffles can decrease the length of the reactor in around 57.5 % for both reactors, this behavior can be seen in Figure 25.

Moreover, when considering the length difference between rectors, the adiabatic one has a bigger value when compared with the GCR. This happens because, as seen Section 4.1.2, the outlet temperature of the adiabatic reactor is higher, but the gases inside the tubes in both reactors need to be cooled to a temperature on 140 °C, therefore, a bigger length is necessary to reach the heat exchange desired. Also, when the GCR is used, there is heat exchange happening in the catalytic reactor, so the temperature ate the outlet of the reactor in the shell side, T_{c2}, is lower.

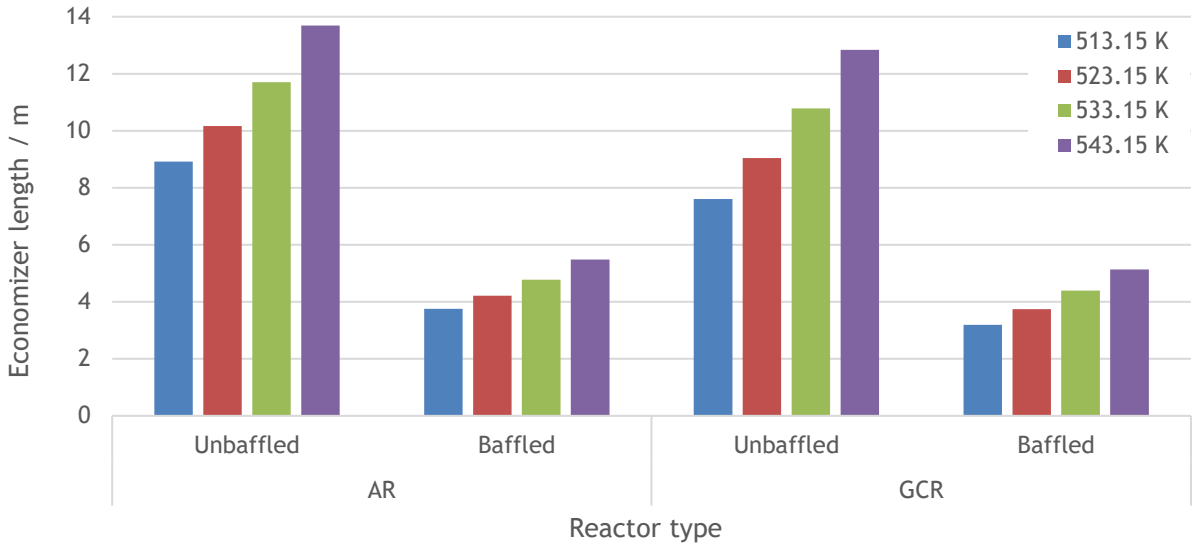

Figure 25: Length of the economizer varying with the inlet temperature for both reactor types with 1000 tubes using a baffled and unbaffled economizer.

Furthermore, the length is lower at small inlet temperature, because, as seen in Section 4.1.2, the outlet temperature is also lower, therefore, less heat needs to be exchanged to reach 140 °C.

Table 13 contains a summary of the decrease in length when the GCR is used instead on the AR for each temperature.

Table 13: Decrease in the economizer length for changing from AR to GCR for each temperature.

	Inlet temperature / K			
	543	533	523	513
ΔL_e **/ %**	6.27	7.94	11.20	14.82

4.2.3 Pressure Drop

Figure 26 represents pressure drop for the cases varying the number of tubes and the inlet temperature for both baffled and unbaffled economizers. Also, this analysis will be made only for the adiabatic reactor, the difference between the pressure drop for both reactors can be as seen in Appendix B.

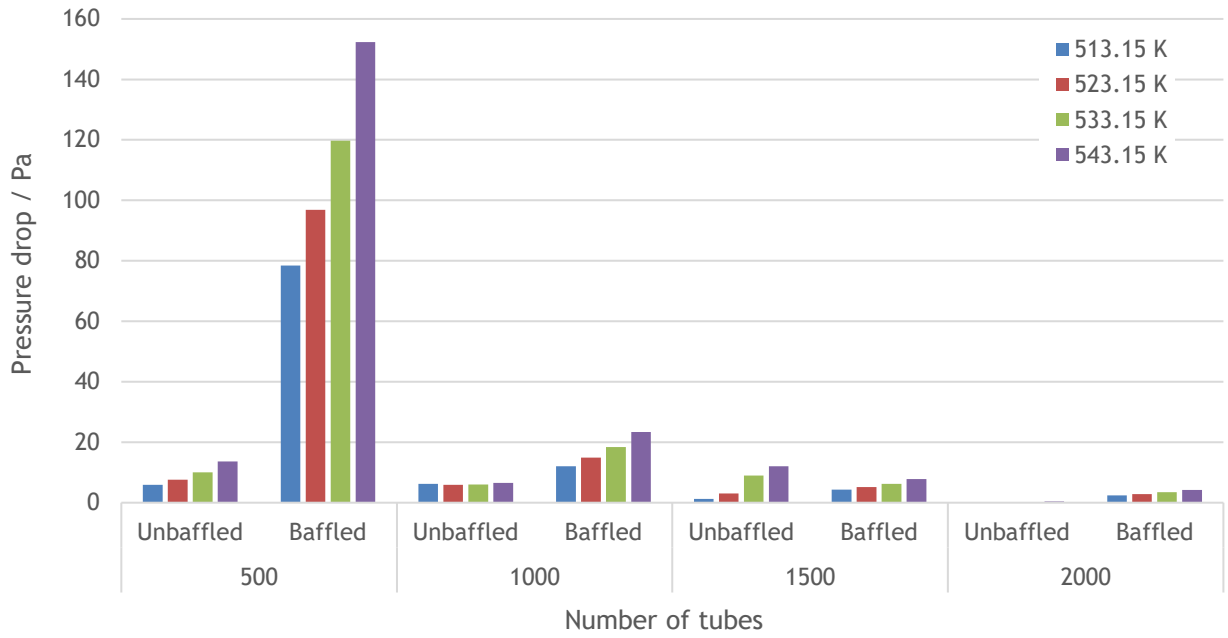

Figure 26: The pressure drop varying with the inlet temperature and the number of tubes in a baffled and unbaffled economizer.

As the flow becomes more turbulent with the baffles, the pressure drop is increased when compared with the unbaffled economizer. Besides that, it can be seen that the behavior of the pressure drop, regarding the range of quantity of tubes studied, has a similar pattern as the one in the catalytic reactor, as seen in Section 4.1.7, since the recycle ratio is approximately 0.85 for all cases studied, as stated in Section 4.1.2.

Also, considering the temperature variation, as high inlet temperatures are followed by higher flowrates, it increases the velocity inside the reactor and, therefore, the turbulence, creating a more pressure drop.

4.2.4 Ratio Between Full Reactor Length and Diameter

The total length, L_t, considering the sum of the lengths of the catalytic reactor and the economizer for the adiabatic reactor and the gas cooled reactor, respectively, are given in Table 14 and 15, this analysis was made varying the number of tubes, presence of baffles and the inlet temperature.

Table 14: Sum of the length of the catalytic reactor with the length of the economizer, in meters, for the AR varying the number of tubes and the inlet temperature.

T_{in} / K	Number of tubes							
	2000		1500		1000		500	
	Unbaffled	Baffled	Unbaffled	Baffled	Unbaffled	Baffled	Unbaffled	Baffled
543	14.8	7.08	15.0	7.12	15.4	7.15	16.1	7.93
533	12.9	6.37	13.1	6.45	13.5	6.55	14.3	7.37
523	11.6	5.94	11.8	6.08	12.3	6.37	13.8	7.79
513	10.6	5.76	10.9	5.96	11.6	6.47	13.6	8.41

Table 15: Sum of the length of the gas cooled reactor with the length of the economizer, in meters, for the GCR varying the number of tubes and the inlet temperature.

T_{in} / K	Number of tubes							
	2000		1500		1000		500	
	Unbaffled	Baffled	Unbaffled	Baffled	Unbaffled	Baffled	Unbaffled	Baffled
543	14.3	6.85	14.4	6.84	14.5	6.80	14.7	7.40
533	12.3	6.11	12.4	6.14	12.6	6.17	12.9	6.82
523	10.9	5.63	11.0	5.70	11.2	5.89	11.9	7.06
513	9.83	5.38	9.95	5.51	10.3	5.91	11.6	7.62

When using baffles, the full length of both catalytic and economizer sections decreases in around 48.3%.

Considering the ratio between these lengths above and the inner shell diameter, and calculating a mean value regarding the inlet temperatures, Table 16 is created.

Table 16: Ratio between the sum of the economizer and catalytic reactor lengths and the shell diameter.

Reactor type	Number of tubes							
	2000		1500		1000		500	
	Unbaffled	Baffled	Unbaffled	Baffled	Unbaffled	Baffled	Unbaffled	Baffled
GCR	1.58	0.80	2.11	1.07	3.22	1.64	6.74	3.93
AR	1.66	0.84	2.25	1.13	3.50	1.77	7.63	4.27

5 Conclusion

This thesis provides a full model and simulation in MATLAB and Aspen Plus of LOGIC reactor for the commercial production of methanol. Furthermore, a comparative analysis was performed by changing parameters such as inlet temperature, number of tubes, catalytic reactor type and presence of baffles. Therefore, all the goals set in this work were completed, providing a good understanding of how the reactor works and how the varied parameters would affect its the design and performance.

As for the chosen parameters, first, the reactor type chosen was the gas cooled, as it provides the highest methanol conversion with the best temperature control, smaller reactor length, lower catalyst weight load and pressure drop. Secondly, the baffled economizer was selected, as it increases the heat exchange by promoting more turbulence in the flow requiring smaller heat exchange area and, therefore, decreasing its length.

For the number of tubes, the quantities of 500 and 2000 should be avoided, the first because it causes the reactor to be too long with a small shell diameter and also promotes the highest pressure drops. The second, 2000 tubes, leads to poor heat exchange and high amounts of catalyst weight, also biggest shell diameter that creates low values of L_t/D_s. The chosen number of tubes was 1000, as it provides almost the same total length and catalyst weight as the 1500 tubes, but with the smaller shell diameter and higher heat exchange, the downside is that it causes a higher pressure drop.

Finally, the inlet temperature chosen was 513.15 K, as it required the lowest inlet mass flowrates, recycle ratios, pressure drops and reactor lengths, while providing the highest conversions, leading to a more efficient methanol production. The disadvantage is that it requires higher amounts of catalyst among the other inlet temperatures considered, but as it is the lowest of them all, the catalyst is less likely to suffer deactivation by sintering, which expands its lifetime.

The final design of the reactor consists in a reactor with 5.9 m of length and 3.7 m of inner shell diameter, with a conversion of 7.7 %, producing 586 $kg\,h^{-1}$, recycle ratio of 0.82, total inlet mass flowrate of 1.63 $kg\,s^{-1}$, requiring only 0.27 $kg\,s^{-1}$ of fresh feed. All or this while needing 1072 kg of catalyst and keeping a reasonable heat transfer and pressure drop.

Overall, the accomplishments of this dissertation have a great impact within DMT Environmental Technology, as it allows them to have a bigger domain and understanding of the LOGIC reactor. Moreover, it provides the company a great opportunity to continue investing in a such promising market as the methanol production.

6 Assessment of the Work Done

6.1 Objectives Achieved

The two-step goal to designing a LOGIC reactor for the commercial production of methanol was achieved. The first being fulfilled by successfully modeling the reactor, implementing it on MATLAB and Aspen Plus, simulating and generating results that agreed with the theory. After that, the data was analyzed, an efficient methanol production was achieved and a design was chosen.

Given that DMT decided to keep inventing in the LOGIC reactor for the production of methanol from renewable sources, it is an indicative that they consider the project to be worth investing in and that the objective proposed were achieved. This project is the first chapter of the development of this technology inside the company and has a lot of potential to grow and to be improved in the following studies.

6.2 Other Work Carried Out

Besides developing the dissertation here presented, I was involved directly with the DMT consortium with UT Twente, ISPT and Shell to build a pilot plant of the LOGIC reactor, participating in the meetings and in the decisions regarding the development of the project.

6.3 Final Assessment

I am thankful for being part of this project that helped me consolidate the extensive knowledge learned from different courses at the university in order to solve the challenges and achieve my goals. Moreover, I learned how the day-to-day life at DMT is like and always felt like they valued my opinions and trusted my work.

From a technical point of view, I believe the LOGIC reactor has a great potential, but a cost analysis should be performed considering the data collected to verify if is financially viable and if the final design chosen has the best cost-benefit ratio.

7 References

- Alarifi, A. *et al*. 'Multiobjective optimization of methanol synthesis loop from synthesis gas via a multibed adiabatic reactor with additional interstage CO2 Quenching', *Energy and Fuels*, 29(2), pp. 530–537. (2015) doi: 10.1021/ef502073b.
- Bertau, M. *et al*. *Methanol: The basic chemical and energy feedstock of the future: Asinger's vision today*, *Methanol: The Basic Chemical and Energy Feedstock of the Future: Asinger's Vision Today*. (2014) doi: 10.1007/978-3-642-39709-7.
- Bos, M. J. *et al*. '110th Anniversary: Characterization of a Condensing CO2 to Methanol Reactor', *Industrial and Engineering Chemistry Research*, 58(31), pp. 13987–13999. (2019) doi: 10.1021/acs.iecr.9b02576.
- Bos, M. J. and Brilman, D. W. F. 'A novel condensation reactor for efficient CO2 to methanol conversion for storage of renewable electric energy', *Chemical Engineering Journal*, 278(1), pp. 527–532. (2015) doi: 10.1016/j.cej.2014.10.059.
- Bozzano, G. and Manenti, F. 'Efficient methanol synthesis: Perspectives, technologies and optimization strategies', *Progress in Energy and Combustion Science*, 56, pp. 71–105. (2016) doi: 10.1016/j.pecs.2016.06.001.
- Churchill, S. W. and Bernstein, M. 'A correlating equation for forced convection from gases and liquids to a circular cylinder in crossflow', *Journal of Heat Transfer*, 99(2), pp. 300–306. (1977) doi: 10.1115/1.3450685.
- Dalena, F. *et al*. (2018) *Methanol Production and Applications: An Overview*, *Methanol: Science and Engineering*. Elsevier B.V. (2018) doi:10.1016/B978-0-444-63903-5.00001-7.
- DMT Environmental Technology. Available in: https://www.dmt-et.com/. Acessed in 14/01/2021
- Ergun, S. 'Fluid flow through packed columns', *Chem. Eng. Prog.*, 48(2), pp. 89–94. (1952) doi: citeulike-article-id:7797897.
- Gmehling, J., Kolbe, B., Kleiber, M., Rarey, J.. Chemical Thermodynamics. Wiley VCH.(2012)
- Graaf, G. H. *et al*. 'Intra-particle diffusion limitations in low-pressure methanol synthesis', *Chemical Engineering Science*, 45(4), pp. 773–783. (1990) doi: 10.1016/0009-2509(90)85001-T.
- Graaf, G. H. and Winkelman, J. G. M. 'Chemical Equilibria in Methanol Synthesis Including the Water-Gas Shift Reaction: A Critical Reassessment', *Industrial and Engineering Chemistry Research*, 55(20), pp. 5854–5864. (2016) doi: 10.1021/acs.iecr.6b00815.

- Graboski, M. S. and Daubert, T. E. 'A Modified Soave Equation of State for Phase Equilibrium Calculations. 3. Systems Containing Hydrogen', *Industrial and Engineering Chemistry Process Design and Development*, 18(2), pp. 300–306. (1979) doi: 10.1021/i260070a022.
- J. M. Smith, H. C. Van Ness, M. M. A. 'Introdução à Termodinâmica de Engenharia Química - 7ªed - Smith, Van Ness, Abbott.pdf', p. 626. (2007)
- Kern, D. Q. 'Process heat transfer', *Journal of the Franklin Institute*, pp. 462–463. (1950) doi: 10.1016/0016-0032(50)90609-0.
- Leonzio, G. 'State of art and perspectives about the production of methanol, dimethyl ether and syngas by carbon dioxide hydrogenation', *Journal of CO2 Utilization*, 27(June), pp. 326–354. (2018) doi: 10.1016/j.jcou.2018.08.005.
- Márquez, C. 'Methanol Report Renewable Methanol Report Authors ':, pp. 1–26. (2018) Available at: www.methanol.orgwww.methanol.org.
- Mathias, P. M. 'A Versatile Phase Equilibrium Equation of State', *Industrial and Engineering Chemistry Process Design and Development*, 22(3), pp. 385–391. (1983) doi: 10.1021/i200022a008.
- Matsumoto, H. *et al*. 'Advanced technology for large scale methanol plant', *Technical Review - Mitsubishi Heavy Industries*, pp. 58–62. (1997)
- Meyer, J. J. *et al*. 'Modeling of a Methanol Synthesis Reactor for Storage of Renewable Energy and Conversion of CO2 - Comparison of Two Kinetic Models', *Chemical Engineering and Technology*, 39(2), pp. 233–245. (2016) doi: 10.1002/ceat.201500084.
- Olah, G. A. 'Beyond oil and gas: The methanol economy', *Angewandte Chemie - International Edition*, 44(18), pp. 2636–2639. (2005) doi: 10.1002/anie.200462121.
- Ott, J. *et al*. 'Methanol - An Industrial Review by Lurgi GmbH, Air Liquide GmbH and BASF AG', *Ullmann's Encyclopedia of Industrial Chemistry*. (2012)
- Palmer, G. and Floyd, J. (2020) *Hydrogen as an energy carrier*, *Lecture Notes in Energy*. (2020) doi: 10.1007/978-3-030-33093-4_8.
- Perry, S. *et al*. *Perry's chemical engineers' handbook*, *Choice Reviews Online*. (2000) doi: 10.5860/choice.38-0966.
- Poling, B.E., Prausnitz, J.M., O'connell, J.P., et al.. The Properties of Gases and Liquids, vol. 5. Mcgraw-Hill, New York. (2001)
- Rezaie, N. *et al*. 'A comparison of homogeneous and heterogeneous dynamic models for industrial methanol reactors in the presence of catalyst deactivation', *Chemical Engineering and Processing: Process Intensification*, 44(8), pp. 911–921. (2005) doi: 10.1016/j.cep.2004.10.004.
- Sadik Kakaç, Hongtan Liu, A. P. 'Heat exchangers: selection, rating, and thermal design', *Choice Reviews Online*, 36(01), pp. 36-0348-36–0348. (1998) doi:

10.5860/choice.36-0348.

- Schmidt, K. G. *M1 Heat Transfer to Finned Tubes*, *VDI Heat Atlas*. (2010) doi: 10.1007/978-3-540-77877-6_94.
- Serna, M. and Jiménez, A. 'A compact formulation of the Bell-Delaware method for heat exchanger design and optimization', *Chemical Engineering Research and Design*, 83(5 A), pp. 539–550. (2005) doi: 10.1205/cherd.03192.
- Smith, J. M. *Chemical Engineering Kinetics*, *Applied Catalysis*. (1981) doi: 10.1016/0166-9834(81)80078-4.
- Soave, G. 'Equilibrium constants from a modified Redlich-Kwong equation of state', *Chemical Engineering Science*, 27(6), pp. 1197–1203. (1972)doi: 10.1016/0009-2509(72)80096-4.
- TEMA 'Standards of the Tubular Exchanger Manufacturers Association. TEMA. 9th Edition. 2007.
- Thome, J. R. *Engineering Data Book III*, *Wieland AG*. (2016) Available at: www.pp-publico.de.
- Tijm, P. J. A., Waller, F. J. and Brown, D. M. 'Methanol technology developments for the new millennium', *Applied Catalysis A: General*, 221(1–2), pp. 275–282. (2001) doi: 10.1016/S0926-860X(01)00805-5.
- Vanden Bussche, K. M. and Froment, G. F. 'A steady-state kinetic model for methanol synthesis and the water gas shift reaction on a commercial Cu/ZnO/Al2O3 catalyst', *Journal of Catalysis*, 161(1), pp. 1–10. (1996) doi: 10.1006/jcat.1996.0156.
- Van Bennekom, J. G. *et al*. 'Modeling and experimental studies on phase and chemical equilibria in high-pressure methanol synthesis', *Industrial and Engineering Chemistry Research*, 51(38), pp. 12233–12243. (2012) doi: 10.1021/ie3017362.
- Watson, T. and Robinson, H. E. 'Thermal Conductivity of a Sample of Type 316 Stainless Steel', *National Bureau of Standards Report*. (1963)
- Yaws, C. L. Heat Capacity of Gas. In *Chemical Properties Handbook*; McGraw-Hill, (1999).

Annex A - Supporting Information

This Annex contains information over the characteristic of the catalyst as well as equations and parameters used to determine gas mixture properties, such as gas density, specific heat capacity, viscosity and thermal conductivity. It can also be found the equations for the enthalpy of reaction, thermal heat conductivity of the reactor's wall and the values of molecular weight of each component considered in Table A.1.

Table A.1: Molecular weight of the components.

	CO	CO_2	H_2	H_2O	CH_3OH	CH_4
MW / kg mol^{-1}	0.028	0.044	0.002	0.018	0.032	0.016

The density of the gas mixture can be obtained with the use of the equation of state resulting in Equation A.1.(Gmehling, 2021)

$$\rho_g = \frac{P}{Z \mathrm{R_g} T} \sum_{i=1}^{\mathrm{NC}} (y_i \, \mathrm{MW_i}) \tag{A.1}$$

The mixing rule of the heat capacity is given by in Equation A.2, while the gas heat capacity for each component can be calculated with Equation E.3. All the coefficients can be found in Table A.2.

$$Cp_g = \frac{\sum_i^{NC} y_i \, Cp_{g,i}(T)}{\sum_i^{NC} y_i \, \mathrm{MW_i}} \tag{A.2}$$

$$Cp_{g,i}(T) = \mathrm{A_{Cp_{g,i}}} + \mathrm{B_{Cp_{g,i}}} T + \mathrm{C_{Cp_{g,i}}} T^2 + \mathrm{D_{Cp_{g,i}}} T^3 \tag{A.3}$$

Table A.2: Coefficients for the specific heat calculation.(Yaws,1999)

	CO	CO_2	H_2	H_2O	CH_3OH	CH_4
$\mathbf{A_{Cp_{g,i}}}$ **/ J mol^{-1} K^{-1}**	30.87	19.80	27.14	32.24	21.15	19.25
$\mathbf{B_{Cp_{g,i}}}$ **/ J mol^{-1} K^{-2}**	-1.28 10^{-2}	7.34 10^{-2}	9.27 10^{-2}	1.92 10^{-3}	7.09 10^{-2}	5.21 10^{-2}
$\mathbf{C_{Cp_{g,i}}}$ **/ J mol^{-1} K^{-3}**	2.79 10^{-5}	-5.60 10^{-5}	-1.38 10^{-5}	1.05 10^{-5}	2.59 10^{-5}	1.20 10^{-5}
$\mathbf{D_{Cp_{g,i}}}$ **/ J mol^{-1} K^{-4}**	-1.28 10^{-8}	1.71 10^{-8}	7.64 10^{-9}	3.60 10^{-9}	-2.85 10^{-8}	-1.13 10^{-8}

Regarding the thermal conductivity and viscosity their mixing rule are expressed by Equations A.4 and A.5, respectively. (Poling et al., 2001).

$$k_f = \sum_{i}^{\mathrm{NC}} \frac{y_i \, k_{fi}(T)}{\sum_j^{NC} y_j \, \Phi_{i,j}(T)} \tag{A.4}$$

$$\mu_g = \sum_{i}^{\mathrm{NC}} \frac{y_i \, \mu_{gi}(T)}{\sum_j^{NC} y_j \, \Phi_{i,j}(T)} \tag{A.5}$$

The pure component expressions of the thermal conductivity and viscosity are calculated with Equations A.6 and A.7, respectively, and their coefficients are given in Table A.3.

$$k_{fi} = \mathrm{A_{kf,i}} + \mathrm{B_{kf,i}} T + \mathrm{C_{kf,i}} T^2 \tag{A.6}$$

$$\mu_{gi} = \mathrm{A_{\mu g,i}} + B_{\mu g,i} T + C_{\mu g,i} T^2 \tag{A.7}$$

While $\Phi_{i,j}$ is given by Equation A.8. (Poling et al., 2001).

$$\Phi_{i,j}(T) = \frac{\left[1 + \left(\frac{\mu_{gi}}{\mu_{gj}}\right)^{1/2} \left(\frac{MW_j}{MW_i}\right)^{1/4}\right]^2}{\sqrt{8\left(1 + \frac{MW_i}{MW_j}\right)}} \tag{A.8}$$

Table A.3: Coefficients for the thermal conductivity and viscosity calculations.

	CO	**CO_2**	**H_2**	**H_2O**	**CH_3OH**	**CH_4**
$\mathbf{A_{\mu g,i}}$	$3\ 10^{-6}$	$-8\ 10^{-7}$	$3\ 10^{-6}$	$4\ 10^{-7}$	$-3\ 10^{-6}$	$8\ 10^{-7}$
$\mathbf{B_{\mu g,i}}$	$6\ 10^{-8}$	$6\ 10^{-8}$	$2\ 10^{-8}$	$3\ 10^{-8}$	$5\ 10^{-8}$	$4\ 10^{-8}$
$\mathbf{C_{\mu g,i}}$	$-2\ 10^{-11}$	$-2\ 10^{-11}$	$-5\ 10^{-12}$	$-4\ 10^{-13}$	$-2\ 10^{-11}$	-10^{-11}
$\mathbf{A_{kf,i}}$	$1.1\ 10^{-2}$	$-1.2\ 10^{-2}$	$-1.8\ 10^{-2}$	$-1.2\ 10^{-2}$	$6.7\ 10^{-3}$	$2.5\ 10^{-3}$
$\mathbf{B_{kf,i}}$	$5\ 10^{-5}$	10^{-4}	$7\ 10^{-4}$	$9\ 10^{-5}$	$-3\ 10^{-5}$	$9\ 10^{-5}$
$\mathbf{C_{kf,i}}$	10^{-8}	10^{-8}	$-4\ 10^{-7}$	$4\ 10^{-8}$	$2\ 10^{-7}$	10^{-7}

The ideal enthalpy for the reactions at a given temperature can be determined by Equation A.9 using the data in Table A-1.(J. M. Smith, H. C. Van Ness, 2007)

$$\Delta H^r = \Delta H^r_{298} + \int_{298}^{T} Cp_g \, \mathrm{d}T \tag{A.9}$$

For the temperature dependent thermal conductivity of the tube wall, Equation A.10 was used. (Watson and Robinson, 1963)

$$k_w = 13.33 + 17.27\frac{T - 273.15}{1000} - 4.334\left(\frac{T - 273.15}{1000}\right)^2 + 3.32\left(\frac{T - 273.15}{1000}\right)^3 \tag{A.10}$$

In Table A.4, it is summarized the characteristics of the $Cu/ZnO/Al_2O_3$ catalyst considered.

Table A.4: Characteristics of the $Cu/ZnO/Al_2O_3$ catalyst.

Shape	Cylinder
Particle density / $kg_{cat}\,m^{-3}$	1 299
Bed density / $Kg\,m^{-3}$	779.5
Bed voidage	0.4

From that, the weight load of the catalyst can be calculated with equation A.11.

$$W_{cat} = L_r \frac{\pi\, d_i^2}{4}\, \rho_b\, N_t \tag{A.11}$$

Appendix A - MATLAB Codes

The programs developed in MATLAB to simulate the catalyst reactor and the economizer of the LOGIC reactor can be found in this appendix. It consists in three main programs and ten functions. The codes will be written considering the reactors with 1000 tubes and 513.15 K.

1.1 Fresh Feed

Main Program to simulate the only the Fresh Feed stream in the adiabatic catalytic reactor to obtain the first estimative of the recycle stream.

```
%Changeable variables
Nt=1000; %Number of tubes
Mtotal = 1.63; %Total mass flowrate - kg/s
w=[0.00001 0.877 0.12 0.00001 0.00001 0.00297]; %Fresh feed mass fraction
T=513.15; %Inlet temperature - K

%Constants/Inlet
MW=[28 44 2 18 32 16]; %Molecular weight - g/mol
MW2=[0.028 0.044 0.002 0.018 0.032 0.016]; %Molecular weight - kg/mol
P=7500000; %Inlet pressure - Pa

%solve mass and energy balance and pressure drop
zrange=(0:0.01:10); % tube size(high enough to reach thermodynamic eq.) - m
IC=[T,w(2),w(3),w(4),w(1),w(5),w(6),P,Nt,Mtotal]; %Initial conditions
[zsol,varsol]=ode45(@ode_adiabatic,zrange,IC); %ode solver

% %Variables at the end of z

Tcat=varsol(end,1); %T
wcat(2)=varsol(end,2); %wCO2
wcat(3)=varsol(end,3); %wH2
wcat(4)=varsol(end,4); %wH2O
wcat(1)=varsol(end,5); %wCO
wcat(5)=varsol(end,6); %wCH3OH
wcat(6)=varsol(end,7); %wCH4
Pcat=varsol(end,8)/100000; %P
ycat=(wcat./MW)/(sum(wcat./MW));

Molflow=sum((Mtotal.*wcat)./MW2); %Partial mol flowrate mol/s
```

1.2 Adiabatic Reactor

This program simulates the full LOGIC reactor with the adiabatic catalytic reactor.

```
%Changeable variables
Nt=1000; %Number of tubes

Mmix = 1.63; %Total mass flowrate - kg/s
Tinlet=513.15; %Inlet temperature of the fresh feed - K
%Recycled stream data from Aspen - Flash Drum
Mrec =1.359; %Mass flowrate of the recycled stream - kg/s
wrec=[0.078 0.761   0.116   0.006   0.035   0.004 ]; %mass fraction of
recycled stream

%Constants/Inlet
MW=[28 44 2 18 32 16]; %Molecular weight - g/mol
MW2=[0.028 0.044 0.002 0.018 0.032 0.016]; %Molecular weight - kg/mol
T=Tinlet; %Temperature - K
P=7500000; %Inlet pressure - Pa
Mfeed=Mmix-Mrec; %Mass flowrate of the fresh feed stream
wfeed=[0.00001 0.877 0.12 0.00001 0.00001 0.00297]; %Mass fraction of fresh
feed
wmix=(Mrec.*wrec+Mfeed.*wfeed)./Mmix; %Mass fraction of the mixed stream
ymix=(wmix./MW)/(sum(wmix./MW)); %Mol fraction of the mixed stream
SN=(ymix(3)-ymix(2))/(ymix(1)+ymix(2)); %Stoichiometric Number - must be
between 2.01 and 2.1

%solve mass and energy balance and pressure drop
zrange=(0:0.005:8); % tube size (high enough to reach thermodynamic eq.) - m
IC=[T,wmix(2),wmix(3),wmix(4),wmix(1),wmix(5),wmix(6),P,Nt,Mmix]; %Initial
conditions
[zsol,varsol]=ode45(@ode_adiabatic,zrange,IC); %ode solver

% %Variables at the end of the reactor
Tcat=varsol(end,1); %T
wcat(2)=varsol(end,2); %wCO2
wcat(3)=varsol(end,3); %wH2
wcat(4)=varsol(end,4); %wH2O
wcat(1)=varsol(end,5); %wCO
wcat(5)=varsol(end,6); %wCH3OH
wcat(6)=varsol(end,7); %wCH4

i=1;
while abs(varsol(end,6)-varsol(i,6))>0.00005
    Lr=zsol(i);%Length of the reactor tube
    i=i+1;
    if i==length(zsol)
        break;
    end
end

Pcat=varsol(i,8); %P - Pa
ycat=(wcat./MW)/(sum(wcat./MW)); %Mol fraction of the reacted stream
Fp(1,:)=(Mfeed.*wfeed)./MW2; %Partial mol flowrate mol/s
Fp(2,:)=(Mrec.*wrec)./MW2; %Partial mol flowrate mol/s
Fp(3,:)=(Mmix.*wmix)./MW2; %Partial mol flowrate mol/s
Fp(4,:)=(Mmix.*wcat)./MW2; %Partial mol flowrate mol/s
Ft=sum(Fp,2); %Total mol flowrate of the reacted stream - mol/s
yrec=(wrec./MW)/(sum(wrec./MW)); %Mol fraction of the reacted stream
conversion=((Ft(3,1)-Ft(4,1))/Ft(3,1))*100;
cat_weight=(Lr*pi*(0.0254^2)/4)*1299*(1-0.4)*Nt;
```

```
%Economizer
Th1=Tcat; %Th1 is the output temperature of the reactor
Th2=140+273.15; %Th2 is the temperature needed at the inlet of the Flash Drum
Tc1=68+273.15; %Tc1 is the temperature of the Flash's outlet
Tc2=Tinlet; %Tc2 is the same temperature as the inlet of the reactor
(adiabatic reactor)

[deltaP_E,U,Ds,Le,Re]=Economizer(yrec,ycat,Nt,Mmix,Mrec,Th1,Th2,Tc1,Tc2,Pcat)
```

1.3 Gas Cooled Reactor

This program simulates the full LOGIC reactor with the gas cooled catalytic reactor.

```
%Changeable variables
Nt=1000; %Number of tubes
Lr=2.7150;% Size of the reactor, the same as the adiabatic reactor for
comparison

Mmix = 1.63; %Total mass flowrate - kg/s
Tinlet=513.15; %Inlet temperature of the fresh feed - K
%Recycled stream data from Aspen - Flash Drum
Mrec =1.359; %Mass flowrate of the recycled stream - kg/s
wrec=[0.078 0.761   0.116   0.006   0.035   0.004 ]; %mass fraction of
recycled stream

%Constants/Inlet
MW=[28 44 2 18 32 16]; %Molecular weight - g/mol
MW2=[0.028 0.044 0.002 0.018 0.032 0.016]; %Molecular weight - kg/mol
P=7500000; %Inlet pressure - Pa
T=Tinlet;  %Temperature Tube - K
Tshell=Tinlet; %Temperature shell - K
Mfeed=Mmix-Mrec; %Mass flowrate of the fresh feed stream
wfeed=[0.00001 0.877 0.12 0.00001 0.00001 0.00297]; %Mass fraction of fresh
feed
wmix=(Mrec.*wrec+Mfeed.*wfeed)./Mmix; %Mass fraction of the mixed stream
ymix=(wmix./MW)/(sum(wmix./MW)); %Mol fraction of the mixed stream
SN=(ymix(3)-ymix(2))/(ymix(1)+ymix(2)); %Stoichiometric Number - must be
between 2.01 and 2.1

%solve mass and energy balance and pressure drop
zrange=(0:0.005:Lr); % tube size - m
IC=[T,wmix(2),wmix(3),wmix(4),wmix(1),wmix(5),wmix(6),P,Tshell,Mrec,Nt,Mmix];
%Initial conditions
[zsol,varsol]=ode45(@ode_gas_cooled,zrange,IC); %ode solver

%Plots along z
subplot(2,2,1);
plot(zsol,varsol(:,1)) % Temperature vs z
xlabel('z');
ylabel('T bulk');
subplot(2,2,2);
plot(zsol,varsol(:,2)) % wCO2vs z
xlabel('z');
ylabel('w CO2');
subplot(2,2,3);
plot(zsol,varsol(:,9)) % Tshell vs z
```

```
xlabel('z');
ylabel('T Shell');
subplot(2,2,4);
plot(zsol,varsol(:,6)) % wCH3OH vs z
xlabel('z');
ylabel('w CH3OH');

%Variables at the end of z

Tcat=varsol(end,1); %T
wcat(2)=varsol(end,2); %wCO2
wcat(3)=varsol(end,3); %wH2
wcat(4)=varsol(end,4); %wH2O
wcat(1)=varsol(end,5); %wCO
wcat(5)=varsol(end,6); %wCH3OH
wcat(6)=varsol(end,7); %wCH4
Pcat=varsol(end,8); %PPa
Tshellcat=varsol(end,9); %Tshell

ycat=(wcat./MW)/(sum(wcat./MW)); %Mol fraction of the reacted stream
Fp(1,:)=(Mfeed.*wfeed)./MW2; %Partial mol flowrate mol/s
Fp(2,:)=(Mrec.*wrec)./MW2; %Partial mol flowrate mol/s
Fp(3,:)=(Mmix.*wmix)./MW2; %Partial mol flowrate mol/s
Fp(4,:)=(Mmix.*wcat)./MW2; %Partial mol flowrate mol/s
Ft=sum(Fp,2); %Total mol flowrate of the reacted stream - mol/s
yrec=(wrec./MW)/(sum(wrec./MW)); %Mol fraction of the reacted stream
conversion=((Ft(3,1)-Ft(4,1))/Ft(3,1))*100;
cat_weight=(Lr*pi*(0.0254^2)/4)*1299*(1-0.4)*Nt;

%Economizer
Th1=Tcat; %Th1 is the output temperature of the reactor
Th2=140+273.15; %Th2 is the temperature needed at the inlet of the Flash Drum
Tc1=68+273.15; %Tc1 is the temperature of the Flash's outlet
Tc2=Tshellcat; %Tc2 is the final temperature of the shell

[deltaP_E,U,Ds,Le,Re]=Economizer(yrec,ycat,Nt,Mmix,Mrec,Th1,Th2,Tc1,Tc2,Pcat)
```

1.4 Specific heat capacity of the gas mixture

```
function cpg=cp_gas(y,T)

MW=[0.028 0.044 0.002 0.018 0.032 0.016]; %Molecular weight - kg/mol
Cp_cte=[30.87 19.80 27.14 32.24 21.15 19.25; -1.28e-2 7.34e-2 9.27e-2 1.92e-3
7.09e-2 5.21e-2;2.79e-5 -5.6e-5 -1.38e-5 1.05e-5 2.59e-5 1.20e-5;-1.28e-8
1.71e-8 7.64e-9 3.60e-9 -2.85e-8 -1.13e-8];

cpgi=zeros(1,6);
for i=1:6
    cpgi(i)=Cp_cte(1,i)+(Cp_cte(2,i)*T)+(Cp_cte(3,i)*T^2)+(Cp_cte(4,i)*T^3);
end

cpg=sum(y.*cpgi)/sum(y.*MW); %specific heat capacity of the gas - J/(kg K)

end
```

1.5 Economizer

```
function
[deltaP_E,U,Ds,Le,Re,Nb]=Economizer(ys,yt,Nt,mh,mc,Th1,Th2,Tc1,Tc2,Ppa)

%Constants
di= 0.0254; %diametro interno do tubo - m
do= 0.0349; %diametro externo do tubo - m
pt=1.25*do; %Tube pitch

%Pre calculations
dTlmtd=( (Th1-Tc2)-(Th2-Tc1) )/(log( (Th1-Tc2)/(Th2-Tc1) )); %Mean
logarithmic temperature difference
T2=(Th1+Tc2+Th2+Tc1)/4; %Mean of the temperatures - K
kw=13.33+17.27*((T2-273.15)/1000)-4.334*(((T2-273.15)/1000)^2)+3.32*(((T2-
273.15)/1000)^3); %Thermal conductivity of the wall W/(m K)

%Convective heat transfer coefficient for the tube side
T1=(Th1+Th2)/2; %Mean temperature for the tube side

rhogt=gas_density(yt,T1,Ppa); %gas density - kg/m3
cpgt=cp_gas(yt,T1); % Cp of the gas - J / (kg K)
miugt=viscosity(yt,T1); % Gas viscosity - kg/(m s)
kft=thermal_conductivity(yt,T1); %thermal conductivity of the gas W/(m K)

Q=mh*cpgt*(Th1-Th2);
vi=(mh/Nt)/(rhogt*di^2*pi/4); %velocity of the fluid inside the tube - m/s
Pri= cpgt*miugt/kft; % Prandtl number
Rei=rhogt*vi*di/miugt; %Reynolds number
fi=1/(1.82*log(Rei)-1.64)^2; %friction factor
Nui=((Rei-1000)*Pri*((fi/8)^(1/2)))/(1+12.7*((Pri^(2/3))-1)*((fi/8)^(1/2))) ;
%nusselt number
hi=Nui*kft/di; %convective heat transfer coefficient on the tube side - W m-2
K-1

%Convective heat transfer coefficient for the shell side without Baffles
T0=(Tc1+Tc2)/2; %Mean temperature for the shell side - K

rhogs=gas_density(ys,T0,Ppa); %gas density - kg/m3
cpgs=cp_gas(ys,T0); % Cp of the gas - J / (kg K)
miugs=viscosity(ys,T0); % Gas viscosity - kg/(m s)
kfs=thermal_conductivity(ys,T0); %thermal conductivity of the gas W/(m K)
Ds=0.637*sqrt(0.87/0.93)*(pi*do^2*Nt*1.25^2); %Shell diameter - m

vo=mc/(rhogs*(Ds^2*pi/4 - (pi*Nt*do^2)/4)); %gas velocity in the shell side -
m/s
Prd= cpgs*miugs/kfs; % Prandtl number
Dh=(4*((pt^2 * sqrt(3)/4)-(pi*do^2 / 8)))/(pi*do/2);% Hydraulic diameter - m
Red=rhogs*vo*Dh/miugs; %Reynolds number
Nud=0.3+ ( (0.62*(Red^(1/2))*Prd^(1/3))*(1+(Red/282000)^(5/8))^(4/5) )/(
(1+(0.4/Prd)^(2/3))^(1/4) ); %nusselt number
ho(1)=Nud*kfs/Dh;%Convective heat transfer coefficient for the shell side - W
m-2 K-1
fod=(1.58*log10(Red)-3.28)^(-2); %friction factor for the shell side without
Baffles

%Convective heat transfer coefficient for the shell side with Baffles
```

```
B=0.5*Ds; %Baffle spacing - m

%Correction factors for the ideal heat transfer coefficient for the shell
side
As=(Ds-(Ds/pt)*do)*B; %minimum bundle cross flow area
Res=do*mc/(miugs*As); % Reynolds number for the crossflow area
if Res<10
    ca=[1.4 -0.667 0 0];
    cb=[48 -1 0 0];
elseif Res<100
    ca=[1.36 -0.657 0 0];
    cb=[45.1 -0.973 0 0];
elseif Res<1000
    ca=[0.593 -0.477 0 0];
    cb=[4.570 -0.476 0 0];
elseif Res<10000
    ca=[0.321 -0.388 0 0];
    cb=[0.486 -0.152 0 0];
elseif Res<100000
    ca=[0.321 -0.388 1.450 0.519];
    cb=[0.372 -0.123 7 0.5];
end
a=ca(3)/(1+0.14*(Res^ca(4)));
b=cb(3)/(1+0.14*(Res^cb(4)));
ji=ca(1)*(Res^ca(2))*(1.33/(pt/do))^(a);%Colburn j-factor for an ideal tube
bank
hid=ji*cpgs*(mc/As)*(Prd^(-2/3));%ideal heat transfer coefficient for pure
cross flow

ho(2)=hid;%shell side heat transfer coefficient using single segmental
baffles
fos=cb(1)*(Res^cb(2))*(1.33/(pt/do))^(b); %friction factor

%Overall heat transfer coefficient
U = (do/(di*hi) + (do*log(do/di)/(2*kw)) + (1./ho)).^(-1); %W/(m2 K)
Le=Q./(pi.*do.*Nt.*U.*dTlmtd); %HE length - m
Nb=fix(Le(2)/B-1); %number of baffles

%pressure drop
pbi=(2*fos*Nt*(mc/As)^2)/rhogs;


%Total pressure drop

deltaP_E(1,1)=(4*fi*Le(1)*rhogt*vi^2)/(di*2); %pressure drop inside the tube
without Baffles
deltaP_E(2,1)=(4*fod*Le(1)*rhogs*vo^2)/(Dh*2); %pressure drop inside the
shell without Baffles
deltaP_E(1,2)=(4*fi*Le(2)*rhogt*vi^2)/(di*2); %pressure drop inside the tube
with Baffles
deltaP_E(2,2)=pbi; %pressure drop inside the shell with Baffles


Re(1)=Rei;
Re(2)=Red;
Re(3)=Res;
end
```

1.6 Reaction Enthalpy

```
function deltaH = Enthalpy(T)

Cp_cte=[30.87 19.80 27.14 32.24 21.15 19.25; -1.28e-2 7.34e-2 9.27e-2 1.92e-3
7.09e-2 5.21e-2;2.79e-5 -5.6e-5 -1.38e-5 1.05e-5 2.59e-5 1.20e-5;-1.28e-8
1.71e-8 7.64e-9 3.60e-9 -2.85e-8 -1.13e-8];

delta_cp=zeros(1,6);
for i=1:6
    delta_cp(i)=Cp_cte(1,i)*(T-298) + Cp_cte(2,i)*(((T^2)/2)-44402) +
Cp_cte(3,i)*(((T^3)/3)-(26463592/3)) + Cp_cte(4,i)*(((T^4)/4)-1971537604);
end

deltaH(1)=(-49200)+delta_cp(5)+delta_cp(4)-delta_cp(2)-3*delta_cp(3);
deltaH(2)=(41200)+(delta_cp(1)+delta_cp(4)-delta_cp(2)-delta_cp(3));

end
```

1.7 Density of the Gas Mixture

```
function rhog=gas_density(y,T,P)

Rg=8.314; % m3 Pa/K mol
MW=[0.028 0.044 0.002 0.018 0.032 0.016]; %Molecular weight - kg/mol
Pbar=P/100000; %bar

[Z] = Thermodynamics(y,T,Pbar);

rhog=(P/(Z*Rg*T))*sum(y.*MW); %Gas density kg/m3

end
```

1.8 Thermodynamic Equilibrium And Kinetic Constants

```
function [Kteq,k] = kinetic_constats(T)
%Constants
Rg=8.314; % J/(mol K)

Ak=[1.07 3453.38 0.499 6.62e-11 1.22e10 ];
Bk=[36696 0 17197 124119 -94765];

Kteq(1)=(10^((3066/T)-10.592)); %Thermodynamic equilibrium constant
Kteq(2)=1/(10^((-2073/T)+2.029)); %Thermodynamic equilibrium constant

k=zeros(1,6);
for i=1:1:5
    k(i)=Ak(i)*exp(Bk(i)/(Rg*T)); %kinetic constants
end
```

```
end
```

1.9 Mass and Energy Balances and Pressure Drop for the Adiabatic Catalytic Reactor

```
function diffeqs=ode_adiabatic(z,var)

%Constants

di= 0.0254; %inner diameter of the tube - m
Ai=(di^2)*pi/4; % transversal area of the tube - m2
rhocat=1299; %Particle density - kg/m3
eb=0.4; %bed voidage
MW=[0.028 0.044 0.002 0.018 0.032 0.016]; %Molecular weight - kg/mol
dp= 0.004; %particle diameter

%Parameters
T=var(1); %T
massfrac(2)=var(2); %wCO2
massfrac(3)=var(3); %wH2
massfrac(4)=var(4); %wH2O
massfrac(1)=var(5); %wCO
massfrac(5)=var(6); %wCH3OH
massfrac(6)=var(7); %wCH4
Ppa=var(8); %P - Pa
Nt=var(9); %Number of tubes
Mt=var(10)/Nt; %Total mass flowrate per tube - kg/(s tube)

%Pre calculations
Pbar=Ppa/1e5; %P - bar
y=(massfrac./MW)/(sum(massfrac./MW)); %mol fraction
pp=y.*Pbar; %partial pressure - bar

%functions

deltaH = Enthalpy(T); %J/mol
[Kteq,k] = kinetic_constats(T); % Thermodynamic equilibrium constant and
kinetic constants
rhog=gas_density(y,T,Ppa);%Gas density kg/m3
cpg=cp_gas(y,T); %specific heat capacity of the gas - J/(kg K)
miug=viscosity(y,T); % Gas viscosity - kg/(m s)

%Calculated

vi=(Mt)/(rhog*di^2*pi/4); %velocity inside the tube - m/s
Re=rhog*vi*di/miug; %Reynolds number inside the tube

rch3oh=(k(1)*pp(2)*pp(3)*( 1-( (pp(4)*pp(5))/(Kteq(1)*pp(2)*(pp(3))^3) ) )) /
( 1+ k(2)*pp(4)/pp(3)+k(3)*(pp(3))^0.5+k(4)*pp(4) )^3; %CH3OH Reaction rate
mol/(kg s)
rrwgs=(k(5)*pp(2)*( 1-( (Kteq(2)* pp(4)*pp(1))/(pp(2)*pp(3)) ) )) / ( 1+
k(2)*pp(4)/pp(3)+k(3)*(pp(3))^0.5+k(4)*pp(4) ); %RWGS Reaction rate mol/(kg
s)

%Diferential equations
```

```
diffeqs(1,1)=((Ai/(Mt*cpg))*(rhocat*(1-eb)*((-deltaH(1))*rch3oh+(-
deltaH(2))*rrwgs))); %dT/dz

diffeqs(2,1)=-rhocat*(1-eb)*MW(2)*(rch3oh+rrwgs)*Ai/Mt; %dwCO2/dz
diffeqs(3,1)=-rhocat*(1-eb)*MW(3)*(3*rch3oh+rrwgs)*Ai/Mt; %dwH2/dz
diffeqs(4,1)=rhocat*(1-eb)*MW(4)*(rch3oh+rrwgs)*Ai/Mt; %dwH2O/dz
diffeqs(5,1)=rhocat*(1-eb)*MW(1)*(rrwgs)*Ai/Mt; %dwCO/dz
diffeqs(6,1)=rhocat*(1-eb)*MW(5)*(rch3oh)*Ai/Mt; %dwCH3OH/dz
diffeqs(7,1)=0; %dwCH4/dz

diffeqs(8,1)=-(150*(1-eb)/Re + 1.75)*rhog*(1-eb)*(vi^2)/(dp*eb^3); %dP/dz

diffeqs(9,1)=0; %dwNt/dz
diffeqs(10,1)=0; %dwM/dz

end
```

1.10 Mass and Energy Balances and Pressure Drop for the Gas Cooled Catalytic Reactor

```
function diffeqs=ode_gas_cooled(z,var)

%Constants

di= 0.0254; %inner diameter of the tube - m
do= 0.0349; %outer diameter of the tube - m
Ai=(di^2)*pi/4; % transversal area of the tube - m2
rhocat=1299; %Particle density - kg/m3
eb=0.4; %bed voidage
MW=[0.028 0.044 0.002 0.018 0.032 0.016]; %Molecular weight - kg/mol
dp= 0.004; %particle diameter
pt=1.25*do; %Tube pitch

%Parameters
T=var(1); %T
massfrac(2)=var(2); %wCO2
massfrac(3)=var(3); %wH2
massfrac(4)=var(4); %wH2O
massfrac(1)=var(5); %wCO
massfrac(5)=var(6); %wCH3OH
massfrac(6)=var(7); %wCH4
Ppa=var(8); %P - Pa
Tshell=var(9); %Tshell
Mrec=var(10); %Total mass flowrate on the shell side - kg/s
Nt=var(11); %Number of tubes
Mt=var(12)/Nt; %Total mass flowrate per tube - kg/(s tube)

%Pre calculations
Pbar=Ppa/1e5; %P - bar
kw=13.33+17.27*((T-273.15)/1000)-4.334*(((T-273.15)/1000)^2)+3.32*(((T-
273.15)/1000)^3); %Thermal conductivity of the wall W/(m K)
y=(massfrac./MW)/(sum(massfrac./MW)); %mol fraction
pp=y.*Pbar; %partial pressure - bar

%functions
```

```
deltaH = Enthalpy(T); %J/mol
[Kteq,k] = kinetic_constats(T); % Thermodynamic equilibrium constant and
kinetic constants
rhog=gas_density(y,T,Ppa);%Gas density kg/m3
cpg=cp_gas(y,T); %specific heat capacity of the gas - J/(kg K)
miug=viscosity(y,T); % Gas viscosity - kg/(m s)
kf=thermal_conductivity(y,T); %thermal conductivity of the gas W/(m K)

%Calculated

rch3oh=(k(1)*pp(2)*pp(3)*( 1-( (pp(4)*pp(5))/(Kteq(1)*pp(2)*(pp(3))^3) ) )) /
( 1+ k(2)*pp(4)/pp(3)+k(3)*(pp(3))^0.5+k(4)*pp(4) )^3; %CH3OH Reaction rate
mol/(kg s)%
rrwgs=(k(5)*pp(2)*( 1-( (Kteq(2)* pp(4)*pp(1))/(pp(2)*pp(3)) ) )) / ( 1+
k(2)*pp(4)/pp(3)+k(3)*(pp(3))^0.5+k(4)*pp(4) ); %RWGS Reaction rate mol/(kg
s)% ****

%Convective heat transfer coefficient for the shell side

Ds=0.637*sqrt(0.87/0.93)*(pi*do^2*Nt*1.25^2); %Shell diameter - m
vo=Mrec/(rhog*(Ds^2*pi/4 - (pi*Nt*do^2)/4)); %gas velocity in the shell side
- m/s
Pr= cpg*miug/kf; % Prandtl number
Dh=(4*((pt^2 * sqrt(3)/4)-(pi*do^2 / 8)))/(pi*do/2); % Hydraulic diameter - m
Red=rhog*vo*Dh/miug; %Reynolds number
Nud=0.3+ ( (0.62*(Red^(1/2))*Pr^(1/3))*(1+(Red/282000)^(5/8))^(4/5) )/(
(1+(0.4/Pr)^(2/3))^(1/4) ); %nusselt number
ho=Nud*kf/Dh; %Convective heat transfer coefficient for the shell side - W m-
2 K-1

%Convective heat transfer coefficient for the tube side
vi=(Mt)/(rhog*di^2*pi/4); %velocity inside the tube - m/s
Re=rhog*vi*di/miug; %Reynolds number inside the tube
hi=((0.458/eb)*(dp*rhog*vi/miug)^(-0.407)) /
((1/(cpg*Mt/Ai))*((cpg*miug/kf)^(2/3))); %W/(m2 K)

%Overall heat transfer coefficient on the shell side
Ushell = (do/(di*hi) + (do*log(do/di)/(2*kw)) +1/ho )^(-1); %  W/(m2 K)

%Overall heat transfer coefficient on the tube side
Utube = (1/(hi) + (di*log(do/di)/(2*kw)) +di/(do*ho) )^(-1) %  W/(m2 K)

%Diferential equations

diffeqs(1,1)=((Ai/(Mt*cpg))*((pi*di*Utube*(Tshell-T)/Ai)+rhocat*(1-eb)*((-
deltaH(1))*rch3oh+(-deltaH(2))*rrwgs))); %dT/dz
diffeqs(9,1)=-(Ai/(Mt*cpg))*((pi*di*Ushell*(T-Tshell)/Ai)); %dTshell/dz

diffeqs(2,1)=-rhocat*(1-eb)*MW(2)*(rch3oh+rrwgs)*Ai/Mt; %dwCO2/dz
diffeqs(3,1)=-rhocat*(1-eb)*MW(3)*(3*rch3oh+rrwgs)*Ai/Mt; %dwH2/dz
diffeqs(4,1)=rhocat*(1-eb)*MW(4)*(rch3oh+rrwgs)*Ai/Mt; %dwH2O/dz
diffeqs(5,1)=rhocat*(1-eb)*MW(1)*(rrwgs)*Ai/Mt; %dwCO/dz
diffeqs(6,1)=rhocat*(1-eb)*MW(5)*(rch3oh)*Ai/Mt; %dwCH3OH/dz
diffeqs(7,1)=0; %dwCH4/dz

diffeqs(8,1)=-(150*(1-eb)/Re + 1.75)*rhog*(1-eb)*(vi^2)/(dp*eb^3); %dP/dz

diffeqs(10,1)=0; %dmc/dz
diffeqs(11,1)=0; %dnt/dz
diffeqs(12,1)=0; %dmt/dz
```

```
end
```

1.11 Thermal Conductivity of the Gas Mixture

```
function kf=thermal_conductivity(y,T)

MW=[28 44 2 18 32 16]; %Molecular weight - g/mol%
kf_cte=[1.1e-2 -1.2e-2 -1.8e-2 -1.2e-2 6.7e-3 2.5e-3;5e-5 1e-4 7e-4 9e-5 -3e-
5 9e-5; 1e-8 1e-8 -4e-7 4e-8 2e-7 1e-7];
kfi=zeros(1,6);
for i=1:6
kfi(i)=kf_cte(1,i)+kf_cte(2,i)*T+kf_cte(3,i)*T^2;
end
mix=zeros(6,6);
for i=1:6
    for j=1:6
        mix(i,j)=((1+sqrt(kfi(i)/kfi(j))*(MW(j)/MW(i))^(1/4))^2) /
sqrt(8*(1+MW(i)/MW(j)));
    end
end

sumi=0;
sumj=zeros(1,6);

for i=1:6
    for j=1:6
        sumj(i)=sumj(i)+y(j)*mix(i,j);
    end
    sumi=sumi+(y(i)*kfi(i)/sumj(i));
end
kf=sumi;

end
```

1.12 Thermodynamics

```
function [Z] = Thermodynamics(y,T,P)

%Constants
Rg=8.314; % J/(mol K)
Tc=[132.9 304.1 33 647.3 512.6 190.4]; %Critica temperature - K
Tr=T./Tc;
Pc=[35 73.8 12.9 221.2 80.9 46]; %Critic pressure - bar
wf=[0.045 0.225 -0.217 0.344 0.565 0.011];
pf=[0 0 0 0.1277 0.2359 0]; %polarity factor
kij=[0 0.1164 -0.0007 -0.474 -0.37 0.0204;0.1164 0 0.1164 0.30 0.10 0.0956;-
0.0007 0.1164 0 -0.745 -0.125 0.001; -0.474 0.30 -0.745 0 -0.075 0.014; -0.37
0.10 -0.125 -0.075 0 0.046; 0.0204 0.0956 0.001 0.014 0.046 0];
NC=6;

mi=0.48508+1.55191.*wf-0.15613.*wf.^2;
alpha=(1+mi.*(1-sqrt(Tr))-pf.*(1-Tr).*(0.7.*Tr)).^2;
```

```
ai=(0.42747.*alpha.*(Rg^2).*(Tc.^2))./Pc;
a=0;

for i=1:1:NC
    for j=1:1:NC
        a=a+y(i)*y(j)*sqrt(ai(i)*ai(j))*(1-kij(i,j));
    end
end

A=(a*P)/(Rg^2*T^2);

bi=0.08664.*Rg.*Tc./Pc;
b=sum(y.*bi);

B=(b*P)/(Rg*T);
auxr1=A-B-B^2;
auxr2=-A*B;
eqn1 =[1 -1 auxr1 auxr2];
ZRoots=roots(eqn1);

Z=max(ZRoots); %Z vapor

end
```

1.13 Viscosity of the Gas Mixture

```
function miug=viscosity(y,T)

MW=[28 44 2 18 32 16]; %Molecular weight - g/mol%
miu_cte=[3e-6 -8e-7 3e-6 4e-7 -3e-6 8e-7;6e-8 6e-8 2e-8 3e-8 5e-8 4e-8; -2e-
11 -2e-11 -5e-12 -4e-13 -2e-11 -1e-11];
miui=zeros(1,6);
for i=1:6
miui(i)=miu_cte(1,i)+miu_cte(2,i)*T+miu_cte(3,i)*T^2;
end
mix=zeros(6,6);
for i=1:6
    for j=1:6
        mix(i,j)=((1+sqrt(miui(i)/miui(j))*(MW(j)/MW(i))^(1/4))^2) /
sqrt(8*(1+MW(i)/MW(j)));
    end
end

sumi=0;
sumj=zeros(1,6);

for i=1:6
    for j=1:6
        sumj(i)=sumj(i)+y(j)*mix(i,j);
    end
    sumi=sumi+(y(i)*miui(i)/sumj(i));
end
miug=sumi;

end
```

Appendix B - Supporting Results

This appendix carries the supporting result for Chapter 4. First, Table B.1 contains the stoichiometric numbers of the reactor's inlet mass flowrate for each temperature.

Table B.1: Stoichiometric numbers.

T_{in} / K	SN
543.15	2.03
533.15	2.03
523.15	2.02
513.15	2.02

As for Table B.2, it presents all the values calculated for pressure drop and Reynolds number in the tube side of the catalytic section.

Table B.2: Values of pressure drop and Reynolds number in the tube side of the catalytic section.

T_{in} / K	Reactor type	Parameters		Number of tubes			
				2000	**1500**	**1000**	**500**
543.15	**AR**	ΔP	Pa	887	2019	6370	45178
		Re	-	2631	3507	5261	10523
	GCR	ΔP	Pa	879	2003	6316	44672
		Re	-	2638	3521	5289	10625
533.15	**AR**	ΔP	Pa	753	1708	5354	36782
		Re	-	2372	3163	4745	9490
	GCR	ΔP	Pa	746	1692	5299	36271
		Re	-	2382	3180	4780	9611
523.15	**AR**	ΔP	Pa	714	1650	5276	39102
		Re	-	2171	2894	4342	8683
	GCR	ΔP	Pa	707	1631	5205	38259
		Re	-	2184	2917	4390	8870
513.15	**AR**	ΔP	Pa	731	1683	5413	40120
		Re	-	1992	2656	3984	7968
	GCR	ΔP	Pa	723	1661	5322	39027
		Re	-	2009	2686	4047	8203

While Table B.3 presents the relative errors for pressure drop and Reynolds number between the adiabatic reactor and the gas cooled reactor still varying number of tubes and inlet temperature. The mean value of the pressure drop is $1.12\% \pm 0.27$ and for Reynolds number is $0.82\% \pm 0.50$.

Table B.3: Relative errors for pressure drop and Reynolds number between the adiabatic reactor and the gas cooled reactor in the tube side of the catalytic section.

T_{in} / K		Error / %			
		2000	1500	1000	500
543.15	ΔP	0.86	0.82	0.84	1.12
	Re	0.29	0.38	0.53	0.96
533.15	ΔP	0.94	0.94	1.02	1.39
	Re	0.41	0.52	0.73	1.26
523.15	ΔP	1.05	1.12	1.34	2.15
	Re	0.60	0.77	1.11	2.14
513.15	ΔP	1.20	1.35	1.68	2.72
	Re	0.87	1.12	1.60	2.95

In Table B.4, it contains all the values calculated for economizer length, pressure drop and Reynolds number in the shell side of the economizer section.

Table B.4: Economizer length, pressure drop and Reynolds number in the shell side of the economizer section.

T_{in} / K	Reactor type			Number of tubes							
				2000		1500		1000		500	
		Baffle		No	Yes	No	Yes	No	Yes	No	Yes
543.15	**AR**	L_e	m	13.87	6.16	13.81	5.94	13.69	5.48	13.17	4.97
		ΔP	Pa	0.42	4.24	12.06	7.83	6.59	23.39	13.68	152.33
		Re	-	59	614	107	1091	248	2456	1102	9823
	GCR	L_e	m	13.36	5.93	13.18	5.66	12.84	5.14	11.79	4.44
		ΔP	Pa	0.40	4.21	13.10	7.78	6.03	23.18	11.95	149.91
		Re	-	59	616	107	1096	250	2471	1114	9931
533.15	**AR**	L_e	m	11.91	5.39	11.82	5.19	11.71	4.77	11.26	4.30
		ΔP	Pa	0.21	3.46	9.02	6.23	6.07	18.40	10.02	119.72
		Re	-	53	549	96	976	222	2195	985	8781
	GCR	L_e	m	11.35	5.13	11.13	4.88	10.78	4.39	9.85	3.76
		ΔP	Pa	0.20	3.43	8.90	6.16	5.38	18.18	8.49	117.27
		Re	-	53	551	96	982	224	2214	999	8906
523.15	**AR**	L_e	m	10.40	4.79	10.29	4.57	10.17	4.21	9.76	3.78
		ΔP	Pa	0.11	2.89	3.00	5.20	5.91	14.88	7.61	96.84
		Re	-	48	498	87	885	201	1991	893	7963
	GCR	L_e	m	9.74	4.48	9.45	4.19	9.04	3.74	7.89	3.04
		ΔP	Pa	0.11	2.85	2.89	5.12	4.92	14.61	5.82	93.54
		Re	-	48	501	87	893	204	2016	915	8155
513.15	**AR**	L_e	m	9.19	4.32	9.05	4.07	8.92	3.76	8.56	3.35
		ΔP	Pa	0.07	2.41	1.25	4.35	6.19	12.05	5.87	78.46
		Re	-	44	452	79	804	183	1809	812	7235
	GCR	L_e	m	8.39	3.93	8.06	3.62	7.61	3.19	6.57	2.56
		ΔP	Pa	0.06	2.37	1.16	4.25	4.76	11.74	4.19	74.98

		Re	-	44	457	80	814	186	1841	837	7463

While Table B.5 presents the relative errors of the pressure drop and Reynolds number between the adiabatic reactor and the gas cooled reactor still varying number of tubes, presence of baffles and inlet temperature. The mean value for Reynolds number is 0.95 % ± 0.55.

Table B.5: Relative errors for pressure drop and Reynolds number between the adiabatic reactor and the gas cooled reactor in the shell side of the economizer section.

T_{in} / K		Error / %							
		2000		1500		1000		500	
	Baffles	No	Yes	No	Yes	No	Yes	No	Yes
543.15	ΔP	3.16	0.61	8.62	0.63	8.50	0.88	12.63	1.58
	Re	0.34	0.34	0.44	0.44	0.61	0.61	1.09	1.09
533.15	ΔP	4.21	0.85	1.27	1.07	11.27	1.21	15.24	2.04
	Re	0.48	0.48	0.60	0.60	0.83	0.83	1.42	1.42
523.15	ΔP	5.81	1.22	3.87	1.57	16.62	1.82	23.47	3.40
	Re	0.69	0.69	0.89	0.89	1.27	1.27	2.40	2.40
513.15	ΔP	8.09	1.74	6.71	2.23	23.19	2.56	28.60	4.42
	Re	0.99	0.99	1.27	1.27	1.80	1.80	3.15	3.15